Zoological Journal of the Linnean Society, 2017, **XX**, 1–29. With 4 figures.

Systematics of the genus *Oecomys* (Sigmodontinae: Oryzomyini): molecular phylogenetic, cytogenetic and morphological approaches reveal cryptic species

Elkin Y. Suárez-Villota[1,2], Ana Paula Carmignotto[3], Marcus Vinícius Brandão[3], Alexandre Reis Percequillo[4] and Maria José de J. Silva[1]*

[1]*Laboratório de Ecologia e Evolução, Instituto Butantan, Av. Vital Brazil, 1500, São Paulo, 05503-900, Brazil*
[2]*Instituto de Ciencias Marinas y Limnológicas, Universidad Austral de Chile, Edificio Emilio Pugín, campus Isla Teja, Valdivia, 5110236, Chile*
[3]*Laboratório de Diversidade Animal, Departamento de Biologia, Universidade Federal de São Carlos, campus Sorocaba, Rodovia João Leme dos Santos, Km 110, Sorocaba, São Paulo, 18052-780, Brazil*
[4]*Departamento de Ciências Biológicas, Escola Superior de Agricultura 'Luiz de Queiroz', Universidade de São Paulo, Av. Pádua Dias, 11, Piracicaba, São Paulo, 13418-900, Brazil*

Received 24 March 2017; revised 22 October 2017; accepted for publication 27 October 2017

Oecomys is a genus of Neotropical arboreal rodents composed of 17 species with diploid number ranging from $2n = 54$ to 86. Despite this high taxonomic and karyotypic diversity, the species-level systematics remains uncertain. We investigated the phylogenetic relationships and species delimitation of *Oecomys* using multiple approaches based on cytogenetic, molecular (mtDNA and nuDNA sequences) and morphological data sets. Sampling included 73 individuals from 25 localities in Amazonia, Cerrado, Pantanal and the Atlantic Forest, as well as 128 DNA sequences from GenBank. Molecular species boundaries associated with karyotype, morphological characters and geographic distribution led us to recognize 15 distinct lineages in *Oecomys*. These include five major well-supported clades composed of *O. bicolor*, *O. catherinae*, *O. cleberi, O. mamorae*, *O. paricola* and *O. roberti*, which were hypothesized as species complexes with at least eight putative new taxa. Three new karyotypes are also reported for the genus: $2n = 54$ (FN = 54), $2n = 62$ (FN = 62) and $2n = 70$ (FN = 74). Sympatry of up to four species with different diploid numbers recovered in distinct clades illustrates the complex evolutionary history in *Oecomys*. These data highlight the importance of combining cytogenetic, morphological and geographic information along with molecular coalescent analyses in developing species delimitation scenarios.

ADDITIONAL KEYWORDS: coalescent models – Cricetidae – integrative approach – molecular systematics – species delimitation.

INTRODUCTION

The tribe Oryzomyini (Cricetidae: Sigmodontinae) currently comprises 34 genera (Weksler, 2006; Percequillo, Weksler & Costa, 2011; Pine, Timm & Weksler, 2012; Weksler, 2015) of which one of the most diverse is *Oecomys* (Carleton & Musser, 2015). This genus is composed of arboreal rodents, distributed throughout southern Central and South America, which are typically associated with tropical lowland rainforests (Musser & Carleton, 2005; Carleton & Musser, 2015). Originally described as a subgenus of *Oryzomys* (Thomas, 1906), subsequent studies elevated *Oecomys* to generic status (Hershkovitz, 1960; Musser & Carleton, 1993) and recognized its monophyly (Smith & Patton, 1993; Patton & Da Silva, 1995; Patton, Da Silva & Malcolm, 2000; Andrade & Bonvicino, 2003; Weksler, 2003, 2006). The phylogenetic relationships among *Oecomys* species, however, have not yet been fully resolved, and few taxa have been assessed in both morphological and molecular analyses (e.g. Weksler, 2006; Rocha *et al.*, 2012; Pardiñas *et al.*, 2016).

*Corresponding author. E-mail: mariajose.silva@butantan.gov.br

Carleton, Emmons & Musser (2009) listed 16 species on the genus *Oecomys*, 12 of which were distributed throughout Brazil (Paglia *et al.*, 2012). Furthermore, a new species from the Chaco Province, Argentina was recently described (Pardiñas *et al.*, 2016), resulting in a total of 17 species. Although these species can be identified by morphological characters (Carleton & Musser, 2015), cytogenetic and molecular analyses have been useful in identifying greater diversity within the genus, which challenges the current taxonomy. As a result, *Oecomys* species complexes have been proposed with possible new and previously undescribed species (Patton & Da Silva, 1995; Patton *et al.*, 2000; Andrade & Bonvicino, 2003; Rocha et al., 2011, 2012; Rosa *et al.*, 2012; Carleton & Musser, 2015). These results suggest that integrative approaches may be required to delimit taxa at species level within *Oecomys*. In fact, cytogenetic analyses show considerable karyological diversity in the genus, with diploid numbers ranging from 54 in *O. rutilus* from northern Amazonas, Brazil (Gomes Júnior *et al.*, 2016) to 86 in *Oecomys* sp. from Rio Juruá in western Amazonas, Brazil (Patton *et al.*, 2000). Thus, high rates of chromosomal variation are associated with species radiation (Gardner & Patton, 1976; Patton *et al.*, 2000). Although chromosomal data were not helpful in species delimitation along with molecular divergence in some cases (Patton *et al.*, 2000), in others, the karyotypes were taxonomically informative in uncovering new species (Langguth, Maia & Mattevi, 2005; Rosa *et al.*, 2012).

Recently, methods using comparative phylogenetic data to delimit species have been proposed (Pons *et al.*, 2006; Knowles & Carstens, 2007; Wiens, 2007; Carstens & Dewey, 2010; Carstens *et al.*, 2013; Rannala, 2015). Some of these use sequence information as the primary information source to establish group membership and define species boundaries, such as the Bayesian General Mixed Yule Coalescent model (bGMYC; Pons *et al.*, 2006; O'Meara, 2010; Fujisawa & Barraclough, 2013) and Bayesian implementation of Poisson Tree Processes (bPTP; Zhang *et al.*, 2013). Other methods analyse multi-locus data sets and require *a priori* assignment of individuals to species categories, such as coalescent-based Species Tree Estimation using the maximum likelihood (STEM; Kubatko, Carstens & Knowles, 2009) or Bayesian Species Delimitation (BSD; Yang & Rannala, 2010). These methods may generate consistent hypotheses for species delimitation in complex genera with conflicting information on species number such as *Oecomys* (e.g. Patton *et al.*, 2000; Rocha *et al.*, 2012; Rosa *et al.*, 2012).

To investigate the phylogenetic relationships and species limits within *Oecomys*, we analysed specimens from Brazilian localities covering distinct biomes, such as the Amazonian Rainforest, Cerrado, Pantanal and Atlantic Forest, as well as sequences from GenBank. We have included 14 currently recognized species in order to provide an overview of the diversity and phylogenetic relationships within the genus. The first approach considers only sequences from one mitochondrial marker [cytochrome *b* (Cyt*b*)] in the phylogenetic analyses and in the bGMYC and bPTP coalescent-based species delimitation methods. Subsequently, phylogenetic relationships of *Oecomys* were reconstructed with a multi-locus data set [Cyt*b* and two nuclear markers: the first exon of interphotoreceptor retinoid-binding protein (IRBP) and intron seven of the beta-fibrinogen (i7FBG)]. STEM and BSD multi-locus methods were also implemented for species delimitation inferences. These phylogenetic and coalescent analyses were integrated with karyology (diploid and fundamental numbers), morphology and geography to support the species delimitation scenario generated for *Oecomys*.

MATERIAL AND METHODS

Sample collection

In total, 73 samples of *Oecomys* were analysed from 25 localities in Brazil (Supporting Information, Table S1). The animals surveyed by the authors were live-trapped and euthanized in the field in accordance with the protocol of Animal Experimentation Ethics (Carpenter, 2012), as well as the Comissão de Ética para Uso de Animais do Instituto Butantan (CEUAIB). Liver and muscle tissues were extracted, preserved in 100% ethanol and stored at –20 °C. The skins, skulls and partial skeletons were deposited in the Brazilian mammal collections of the Museu de Zoologia da Universidade de São Paulo (MZUSP), Museu Nacional, Universidade Federal do Rio de Janeiro (MN), Universidade Federal do Espírito Santo (UFES) and Universidade de Brasília (UNB). Additionally, the samples also included tissues deposited in the collections of the Instituto Butantan, Instituto de Biociências (IBUSP), Museu de Zoologia da Universidade de São Paulo (MZUSP), São Paulo, Museu Nacional (MN) and Laboratório de Biologia e Controle da Esquistossomose, Fundação Instituto Oswaldo Cruz (LBCE - FIOCRUZ), Rio de Janeiro (Supporting Information, Table S1).

We also included 128 Cyt*b* *Oecomys* sequences downloaded from GenBank (Supporting Information, Table S1). The outgroup was composed of 21 sequences: three from GenBank and 18 obtained in this study (Supporting Information, Table S2).

DNA extraction, amplification and sequencing

DNA was extracted from liver or muscle using Chelex following Walsh *et al.* (1991). Partial genes Cyt*b*, IRBP and i7FBG were amplified with PCR using the primers indicated in Table 1. Both extraction and non-template PCR controls were used for each amplification. Each

Table 1. Oligonucleotide primers used to amplify specific fragments of mtDNA (Cyt*b*) and nuDNA (the first exon of IRBP and the i7FBG) sequences in *Oecomys* specimens

Locus	Primer	Sequence	Annealing temperature	Amplified fragment	Source
Cyt*b*	MVZ05	5′-CGA AGC TTG ATA TGA AAA ACC ATC GTT G-3′	48 °C	779 bp	Irwin, Kocher & Wilson (1991)
	MVZ16	5′-AAA TAG GAA RTA TCA YTC TGG TTT RAT-3′			Smith & Patton (1993)
IRBP	A1	5′-ATG CGG AAG GTC CTC TTG GAT AAC-3′	60 °C	752 bp	Stanhope *et al.* (1992)
	F	5′-CTC CAC TGC CCT CCC ATG TCT-3′			Stanhope *et al.* (1992)
i7FBG	Bfib	5′-CAC AAC GGC ATG TTC TTC AGC AC-3′	63 °C	649 bp	Matocq, Shurtliff & Feldman (2007)
	B17	5′-ACC CCA GTA GTA TCT GCC GTT TGG AT-3′			Matocq *et al.* (2007)

Cyt*b*, cytochrome *b*; IRBP, interphotoreceptor retinoid-binding protein; i7FBG, intron seven of the beta-fibrinogen.

PCR mixture contained 30 ng of DNA, 25 pmol of each primer, 0.2 mM of dNTP and 2.52 µL of reaction buffer (50 mM KCl, 2.5 mM $MgCl_2$ and 10 mM Tris–HCl; pH 8.8). To this mixture, 0.2 units of Platinum Taq DNA Polymerase (Invitrogen) were added for a total of 18 µL of PCR reaction mixture. Forty amplification cycles were performed in a thermal cycler (Eppendorf Mastercycler ep Gradient, Model 5341). Each cycle consisted of denaturation at 94 °C for 30 s, annealing (this temperature is indicated in Table 1 for each locus) and extension at 72 °C for 45 s. Final extension at 72 °C for 5 min was performed for all amplifications. The PCR products were visualized using 1% agarose gels in TAE buffer and purification was carried out with an ExoSAP-IT kit (Code number US78200, GE Healthcare).

Nucleotide sequencing was conducted using BigDye (DNA 'Big Dye Terminator Cycle Sequencing Standard', Applied Biosystems) and an ABI PRISM 3100 Genetic Analyzer (Applied Biosystems). Electropherograms were visualized and aligned with CodonCode Aligner software, version 4.1.1. (CodonCode Corporation, Dedham, MA, USA) implementing iterative methods of global pairwise alignment (G-INS-i) (Thompson, Higgins & Gibson, 1994; Edgar, 2004). Sequences were submitted to GenBank under accession numbers MG323616 to MG323852.

Phylogenetic analyses

The phylogenies were reconstructed based on either maximum likelihood (ML) analyses or Bayesian inference (BI) using sequences generated in this work and downloaded from GenBank (Supporting Information, Table S1). Both analyses were carried out using only Cyt*b* sequences (n = 201), a concatenated multi-gene data set with missing data or gaps (all Cyt*b* + i7FBG + IRBP sequences), and a concatenated multi-gene data set without missing data (only sequences exclusively generated in this study with information from the three molecular markers – Cyt*b*, IRBP and i7FBG for each individual; n = 73). The outgroup was composed of *Hylaeamys megacephalus*, *Euryoryzomys lamia*, *E. macconnelli*, *E. nitidus* and *E. russatus* following Weksler (2006; Supporting Information, Table S2). For all phylogenetic analyses, the best-fitting partitioning schemes and models of nucleotide substitution were selected using the Bayesian information criterion (BIC), implemented in PartitionFinder version 1.1.0 (Lanfear *et al.*, 2012). ML analyses were performed using GARLI version 2.0 0 (Bazinet, Zwickl & Cummings, 2014). Three likelihood analyses were performed to ensure convergence of the topologies. Statistical support for the nodes was estimated by nonparametric bootstrapping (Felsenstein, 1985), with 1000 pseudoreplicates. Bayesian analysis was performed using MrBayes 3.04b (Ronquist & Huelsenbeck, 2003). Markov chains were started from a random tree and run for 1.0×10^7 generations, sampling every 1000th generation. The stationary phase was checked following Nylander *et al.* (2004) using Tracer version 1.6 (Rambaut *et al.*, 2014). Sample points prior to the plateau phase were discarded as burn-in and the remaining trees were combined to find the maximum *a posteriori* estimated probability of the phylogeny. Branch supports were estimated with Bayesian posterior probabilities (BPP). Two simultaneous analyses were performed to ensure convergence on topologies. The evolutionary distance between pairs of Cyt*b* sequences was estimated with MEGA version 6.0.6 (Tamura *et al.*, 2013) using the Kimura 2-parameter (K2P) with rate variation among sites and the model was selected based on the BIC.

Coalescent-based species delimitation methods

Species delimitation analyses should be performed using different methods in order to examine whether the delimited groups are consistently recovered under

different parameters (Carstens *et al.*, 2013). Therefore, we used single and multi-locus approaches as follows.

Two single-locus analyses: bGMYC and bPTP for species delimitation were performed for the Cyt*b* sequences downloaded from GenBank and those generated in this study (Supporting Information, Table S1). These coalescent-based species delimitation methods take a genealogy estimated from a single genetic locus as input and attempt to model the transition point between cladogenesis and allele coalescence, based on the assumption that the former would occur at a far lower rate than the latter (Pons *et al.*, 2006; Fujisawa & Barraclough, 2013; Zhang *et al.*, 2013). For bGMYC analysis, we used 100 ultrametric trees reconstructed and calibrated by the Bayesian method using BEAST version 1.8 (Drummond *et al.*, 2012). We used the same nucleotide substitution model as in the phylogenetic analysis with an uncorrelated log-normal relaxed clock and Yule prior. A mutation rate of 0.165 subst/site/MY corresponding to the average of those reported by Nabholz *et al.* (2008) for the *Oecomys* lineage was used as the prior in four independent runs with 2×10^7 generations. We conducted a sampling scheme once every 2000 generations. The first 2000 trees were then discarded from each run and the independent log and tree files were combined using LogCombiner version 1.8 (Drummond *et al.*, 2012). The last 100 trees were used as input data for species delimitation analysis, which was conducted using the R package bGMYC (Reid & Carstens, 2012). bGMYC consisted 250 000 generations with a burn-in of 25 000. For bPTP analysis, a Cyt*b* tree obtained with MrBayes version 3.04b software was used as input on bPTP web server of the Exelixis Lab (http://species.h-its.org).

Two multi-locus coalescent-based methods: STEM (Kubatko *et al.*, 2009; Carstens & Dewey, 2010) and BSD (Yang & Rannala, 2010) were applied for species delimitation using Cyt*b*, IRBP and i7BFG sequences (concatenated data set without gaps). Since the performance of STEM and BSD, when there is a large percentage of missing data, has not been thoroughly investigated, we did not use the concatenated data set with missing data (n = 201) in these analyses. STEM and BSD calculate the best species tree using a likelihood or Bayesian framework to identify the best of many possible scenarios of species delimitation and require the *a priori* assignment of individuals to species category (Kubatko *et al.*, 2009; Carstens & Dewey, 2010; Yang & Rannala, 2010). Thus, we performed a set of analyses where individuals were assigned to a series of alternative species numbers ranging from two to 20 species. These alternative delimitation scenarios were based on groups with the same diploid number, groups with similar geographic distribution or those that were recovered as monophyletic in phylogenetic analyses.

STEM analysis used the Cyt*b*, IRBP and i7BFG gene trees obtained by previous ML analyses. This analysis requires fully resolved gene trees, so polytomies were resolved randomly and internode branch lengths were set to 1.0×10^{-8} using Mesquite version 2.75 (Maddison & Maddison, 2011). Since *theta* ($4N\epsilon\mu$) is provided by the user in STEM analysis, we calculated this value according to recommendations of Harrington & Near (2012). The ML scores for each species tree were generated using STEM version 2.0 (Kubatko *et al.*, 2009) and evaluated using an information-theory approach, as outlined in Carstens & Dewey (2010) and Carstens *et al.* (2013).

BSD analysis was applied using Bayesian Phylogenetics and Phylogeography software version 2.2 (BP&P v. 2.2; Rannala & Yang, 2003; Yang & Rannala, 2010). This method accommodates species phylogeny and lineage sorting due to ancestral polymorphism. A gamma prior G (2, 1000) with a mean of 2/2000 = 0.001 was used for the population size parameters (θs). The age of the root in the species tree (τ0) was assigned the gamma prior G (2, 1000), while the other divergence time parameters were assigned the Dirichlet prior (Yang & Rannala, 2010: equation 2). User-specified guide trees were derived from the BI of the concatenated analyses. The rjMCMC analyses used different starting seeds, 200 000 generations (each fifth sampled), and a burn-in of 10 000, which produced consistent results. Ensuring adequate rjMCMC mixing involves specifying a reversible jump algorithm to achieve dimension matching between species delimitation models with different numbers of parameters. We used algorithm 0 with the fine-tuning parameter e = 5. Additionally, the program was run a few times with e = 10 or 15 for the same algorithm or using algorithm 1 with default fine-tuning parameters (a = 2 and m = 1) to ensure stability among runs.

Cytogenetics

Mitotic plates were obtained *in vivo* from spleen and bone marrow according to Ford & Hamerton (1956) or from primary fibroblast cultures derived from ear tissue following the Freshney (1986) protocol. Conventional Giemsa staining was used to determine the diploid number ($2n$), and C-banding was performed according to Sumner (1972) to visualize heterochromatic regions, define the number of autosome arms (FN) and evidence sex chromosomes. Mitotic plates were digitally captured with visible light on an Axioskop 40 microscope (Carl Zeiss) equipped with an Axiocam camera and AxioVision software. We analysed 50 specimens and at least 20 metaphases from each of the specimens (see examined material in Appendix I).

Morphological analyses

We discarded *a priori* those qualitative traits most affected by age variation and kept those less prone to age variation, in order to increase sample sizes (see Appendix II). Then, we focused on the following qualitative traits: pelage and tail coloration, morphology of the tail, incisive foramina, interorbital region, supraorbital margins, alisphenoid strut, subsquamosal fenestra and carotid circulatory pattern. For these, we followed the definitions used by Hershkovitz (1962), Voss (1988), Weksler (2006) and Carleton & Musser (2015). Nevertheless, we only included the variation assigned to these traits when this proved not to be age dependant (i.e. when young did not differ from adults). We also followed Pardiñas *et al.* (2016) for information regarding *O. franciscorum*.

Quantitative data were obtained only for adult specimens, with all molars fully erupted. We recorded the external measurements on specimen tags, as head and body length (HBL), tail length (TL), hindfoot length (HFL) including claw (all in millimetres) and body mass (W; in grams). We also measured cranial dimensions with digital calipers (to the nearest 0.01 mm). We employed the following cranial measurements as detailed in Voss, Lunde & Simmons (2001): condyle-incisive length (CIL), length of the diastema (LD), crown length of the upper molar series (LM), breadth of first upper molar (BM1), length of the incisive foramina (LIF), breadth of the incisive foramina (BIF), breadth of the palatal bridge (BPB), breadth of the zygomatic plate (BZP), length of the rostrum (LR), length of nasals (LN), interorbital breadth (LIB), breadth across the squamosal zygomatic processes (ZB), breadth of the braincase (BB) and zygomatic length (ZL).

Species and species groups

We used molecular, cytogenetic, morphological and geographic data to delimit species and species groups within the genus *Oecomys*, as the concordance among these complementary approaches provided solid evidence for taxon delimitation. We also compared cytogenetic data from literature (Patton *et al.*, 2000; Andrades-Miranda *et al.*, 2001; Langguth *et al.*, 2005; Asfora *et al.*, 2011) with morphologically characterized specimens with similar karyotypes and/or phylogenetic relationships. Since we did not examine vouchers from sequences downloaded from GenBank, the names used were assigned by the original authors who performed taxonomic identification based on morphological analyses of the vouchers (see Supporting Information, Table S1).

Name attributions to clades, whether species or species groups, were based on morphological comparisons of the specimens assigned to them with the descriptions and characterizations of valid taxa of *Oecomys* (Patton *et al.*, 2000; Voss *et al.*, 2001; Weksler, 2006; Carleton *et al.*, 2009; Asfora *et al.*, 2011; Percequillo *et al.*, 2011; Rocha *et al.*, 2011; Rosa *et al.*, 2012; Carleton & Musser, 2015; Pardiñas *et al.*, 2016). We examined most of the specimens included in the molecular analyses and specimens not sequenced but with similar morphology from nearby regions (see specimens examined in Appendix II). For sequences neither published nor identified at species level in the literature (e.g. Andrade & Bonvicino, 2003; Orozco *et al.*, 2014; Rocha *et al.*, 2015; Miranda *et al*., unpublished data), names were attributed according to their phylogenetic position in the recovered trees, since we had morphologically examined most specimens recovered in the distinct clades (see Supporting Information, Table S1; Appendix II).

RESULTS

Phylogenetic analyses: major lineages and species groups

The best-fitting models selected for phylogenetic analyses with Cyt*b* sequences were TrNef+I+G, F81+I and TrN+I+G for first, second and third codon positions, respectively. The K80+I model was selected for the first and third codon positions of IRBP in a single data block, and HKY+G was the best-fit model for the second codon position of IRBP and i7BFG. These models and partition schemes were the same for concatenated analyses without missing data or gaps (only specimens with Cyt*b* + IRBP + *i*7BFG sequences) and the concatenated analyses with missing data or gaps (using all Cyt*b* + IRBP + *i*7BFG sequences). The ML tree obtained from Cyt*b* analysis had a –ln likelihood score of –8052.082 and exhibited the same topology as the analysis based on concatenated analyses with gaps, which is a super matrix (Fig. 1). The Bayesian analyses using Cyt*b* sequences and super matrix sequences also recovered a consensus topology similar to the ML tree. The topological disagreement was restricted to low-supported branches (Fig. 1). High bootstrap and BPP supports for the major clades of the mtDNA single-gene tree and the super matrix resulted in 15 distinct major lineages in *Oecomys*: **Clade A** – *O. roberti* species group, **Clade B** – *O. bicolor*/*O. cleberi* species group, **Clade C** – *O. mamorae*/*O. franciscorum* species group, **Clade D** – *O. paricola* species group, **Clade E** – *O. catherinae* species group, *O. rex*, *O. auyantepui*, *O. rutilus*, *O. concolor*, *O. sydandersoni*, *O. trinitatis*, *O superans* and three taxa treated as *Oecomys* sp. 1, *Oecomys* sp. 2 and *Oecomys* sp. 3 (Fig. 1). These 15 lineages represented 14 valid species: *O. auyantepui* Tate,

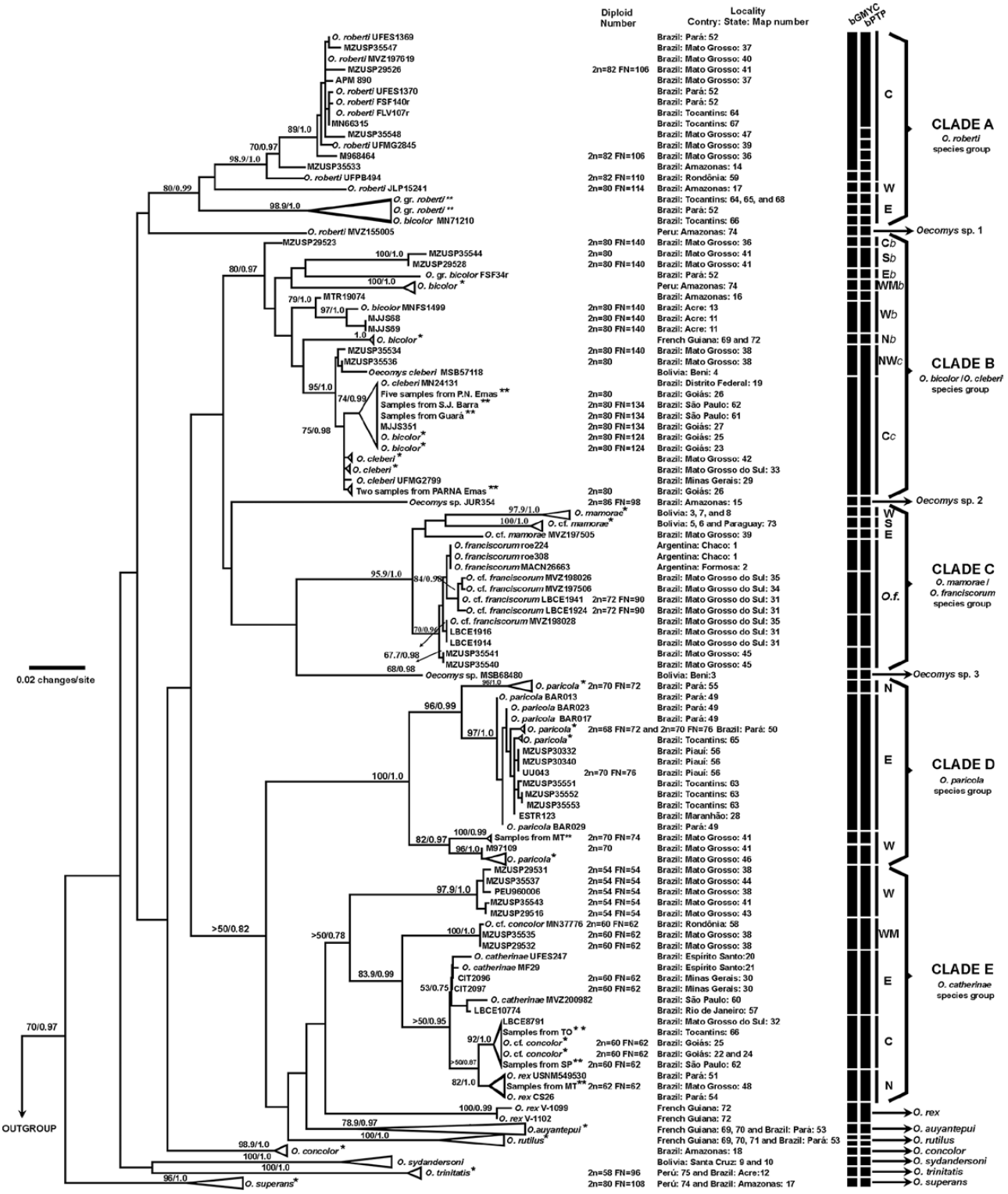

1939; *O. bicolor* (Tomes, 1860); *O. catherinae* Thomas, 1909; *O. cleberi* Locks, 1981; *O. concolor* (Wagner, 1845), *O. franciscorum* Pardiñas, Teta, Salazar-Bravo, Myers & Galliari, 2016; *O. mamorae* (Thomas, 1906); *O. paricola* (Thomas, 1904), *O. rex* Thomas, 1910; *O. roberti* (Thomas, 1904); *O. rutilus* Anthony, 1921; *O. superans* Thomas, 1911; *O. sydandersoni* Carleton, Emmons & Musser, 2009 and *O. trinitatis* (Allen & Chapman, 1893).

Ten of the major lineages are represented exclusively by sequences downloaded from GenBank (Supporting Information, Table S1) as follows: *O. auyantepui* represented by sequences from French Guiana and the state of Pará, Brazil; *O. concolor* from Amazonas, Brazil; *O. rex* from French Guiana; *O. rutilus* from French Guiana and Pará, Brazil; *O. superans* from Peru and Amazonas, Brazil; *O. sydandersoni* from Bolivia; *O. trinitatis* from Peru and Acre, Brazil and three taxa treated as *Oecomys* sp. 1, *Oecomys* sp. 2 and *Oecomys* sp. 3 from Peru, Brazil and Bolivia, respectively. *Oecomys* sp. 1 was treated as *O. roberti* by Carleton *et al.* (2009) (Fig. 1; MVZ 155005, locality 74).

Phylogenetic relationships among the major lineages were not resolved in the Cyt*b* analyses nor in the concatenated analyses with gaps (the super matrix), but an internal structure was recovered for the five major clades (Clades A–E; Fig. 1). However, the concatenated analysis without gaps (Fig. 2) recovered phylogenetic relationships among the five major clades (A–E) with high support values, as well as *Oecomys* monophyly (bootstrap = 87.6% and BPP = 0.99). This analysis corroborates the clades and internal structures recovered in the Cyt*b* tree (Fig. 1; 73 samples + 128 GenBank sequences) and the relationships among them. The Clade E – *O. catherinae* species group was recovered as the sister lineage of two clades: Clade D – *O. paricola* species group as the sister to Clade B – *O. bicolor*/*O. cleberi* species group, which in turn was sister to Clade A – *O. roberti* species group + Clade C – *O. franciscorum*: (Clade E + (Clade D + (Clade B + (Clade A + Clade C)))) (Fig. 2).

The ML and Bayesian tree topologies obtained from single (mtDNA marker; Supporting Information, Fig. S1, left) and concatenated nuclear DNA data sets (Supporting Information, Fig. S1, right) were congruent in recovering Clades B–D (Supporting Information, Fig. S1). Clade A was recovered with high node support values in only the Cyt*b* data set (Supporting Information, Fig. S1, left), and Clade E was recovered with low node support values in both data sets (Supporting Information, Fig. S1). Relationships within the Clade A–D group were also not resolved in these data sets and only the Cyt*b* data set recovered the monophyly of this latter grouping in the BI approach (Supporting Information, Fig. S1, left). *Oecomys* monophyly, however, was recovered in all analyses using single and concatenated data sets (Supporting Information, Fig. S1).

Phylogenetic analyses: relationships within species groups

Clade A (*O. roberti* species group) was highly supported in both ML and BI analyses for the concatenated data sets with and without gaps (Figs 1, 2). The clade is composed of sequences from specimens distributed in Cerrado, Pantanal and western/central Amazonia (Fig. 3A). Within Clade A, two well-supported clades were recovered (both with supports 98.9/1.0 in Fig. 1): one represented by specimens from Pantanal, northwestern Cerrado and central Amazonia (Fig. 3A, central clade) and other by specimens exclusively from the northern Cerrado – eastern clade in Figure 3A, including one specimen from locality 66 treated as *O. bicolor* by Vilela *et al.* (2014) and specimens treated as *Oecomys* gr. *roberti* by Rocha *et al.* (2015). One

Figure 1. Phylogenetic relationships of *Oecomys* specimens using Cyt*b* matrix data set and maximum likelihood (ML) analyses. Bayesian inference (BI) using both Cyt*b* and the concatenated data set with missing data (all Cyt*b* + IRPB + iBF7) showed similar topology. Bootstrap and posterior probability support values are above branches (values above 70% and/or above 0.90, respectively). Diploid and fundamental numbers, country: state/province (number as cited on the maps) and clades A–E are indicated. Black bars (on the right of the tree) indicate the species limits as proposed by Bayesian General Mixed Yule Coalescent (bGMYC) and Bayesian implementation of Poisson Tree Processes (bPTP) analyses. Clades are indicated on the right of the black bars according to Figure 3 as follows: C, central; W, western; S, southern; E, eastern; WM, westernmost; *O. f.*, *O. franciscorum*. In Clade B, *O. bicolor* and *O. cleberi* clades are indicated with letter *b* and *c*, respectively, after the geographic abbreviation in the bar. Taxon name and delimitation were based on multiple approaches (molecular + karyotype + morphology); for details, see 'Discussion'. Taxon names were attributed to sequences downloaded from GenBank. Voucher numbers and the available diploid and fundamental numbers are shown and based on the references listed in Supporting Information, Table S1. Specimens sequenced in this work are cited as voucher numbers. *Collapsed clades composed of sequences downloaded from GenBank, accession numbers shown in Supporting Information, Table S1. **Collapsed clades composed of samples from this study, voucher numbers shown in Supporting Information, Table S1 and in Figure 2.

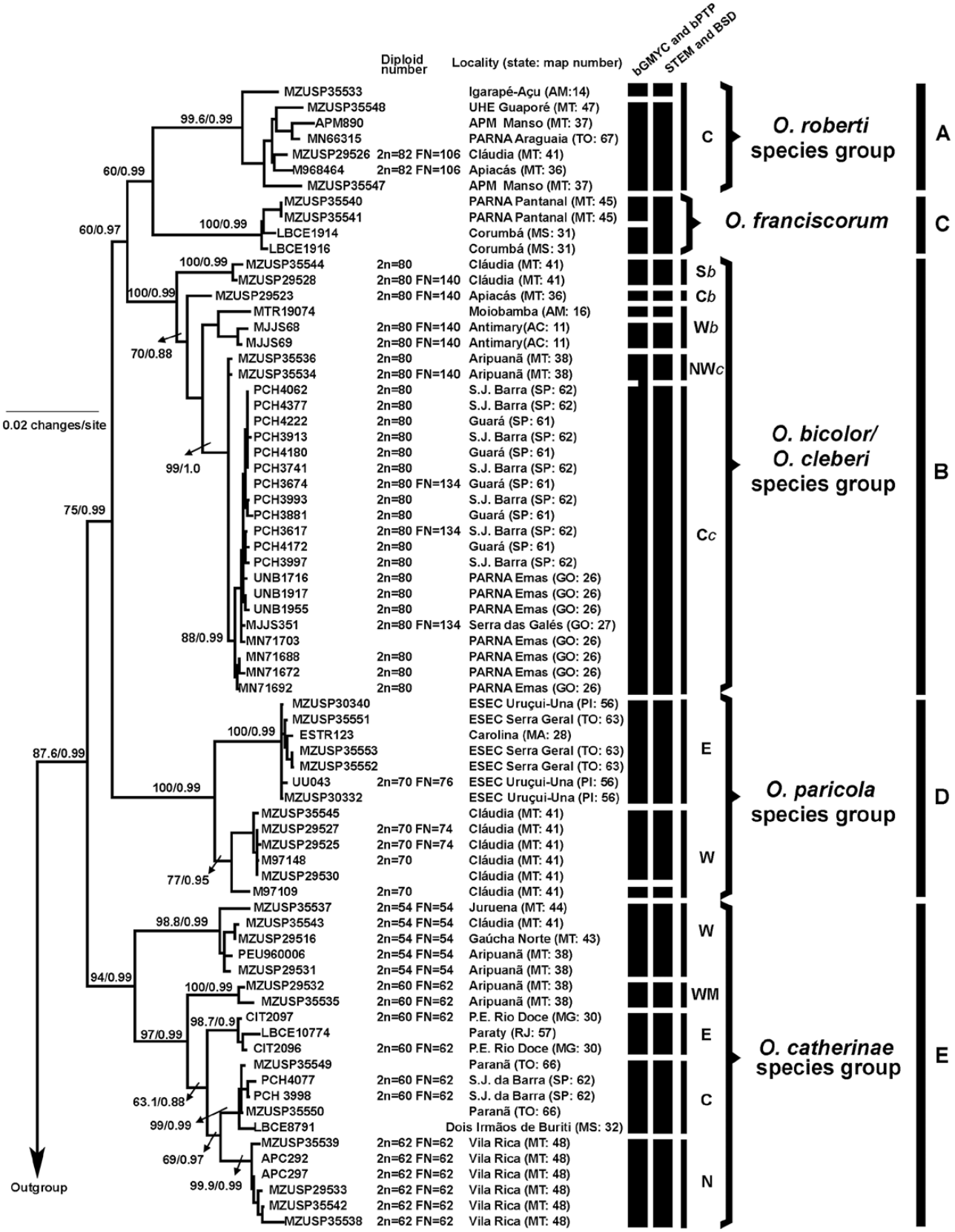

sequence from western Amazonia was also recovered in Clade A (Figs 1, 3A; JLP15241, western clade), but its phylogenetic relationship was not resolved (Fig. 1).

Clade B (*O. bicolor*/*O. cleberi* species group) was well supported in both ML and BI for single-gene and concatenated data sets (Figs 1, 2; Supporting Information, Fig. S1) and was composed of monophyletic lineages distributed along the Amazon and Cerrado biomes (Figs 1, 3B). Specimens treated as *O. bicolor* from the Brazilian Amazon biome (central, eastern, southern and western clades), Peru (westernmost clade) and French Guiana (northern clade) were recovered as highly supported monophyletic clades with unresolved phylogenetic relationships within Clade B (Fig. 1). Specimens treated as *O. cleberi* were recovered as one monophyletic lineage distributed in the Cerrado and southwestern Amazon (Fig. 3B; supports 95/1.0 and 99/1.0 in Figs 1 and 2, respectively). This lineage included one sample from Bolivia treated as *O. cleberi* by Pardiñas *et al.* (2016) and two samples from Mato Grosso, Brazil (Figs 1, 3B; MSB 57118, MZUSP 35534 and MZUSP 35536, northwestern clade). These Amazonian samples were highly related to the Cerrado specimen clade (Figs 1, 3B, central clade) composed of the *O. cleberi* holotype (MN 24131) and its related sequences, studied by Rocha *et al.* (2012). As part of this clade, we also recovered specimens with $2n = 80$, FN = 134 (Fig. 1; specimens from localities 27, 61 and 62) and those treated as *Oecomys* cf. *bicolor* with $2n = 80$, FN = 124 by Andrades-Miranda *et al.* (2001) (Fig. 1; specimens from localities 23 and 25 treated in GenBank as *O. bicolor* by Miranda *et al.*, unpublished data).

Clade C (*O. mamorae*/*O. franciscorum* species group) was highly supported in both ML and BI for single-gene and concatenated data sets (Figs 1, 2; Supporting Information Fig. S1) and was composed of individuals distributed in Brazil (Mato Grosso and Mato Grosso do Sul), Argentina, Bolivia and Paraguay (Fig. 3C). Specimens from northern Bolivia (Fig. 3C, western clade), southern Bolivia and eastern Paraguay (southern clade), and one specimen from western Brazil (eastern clade), were recovered as distinct monophyletic lineages. Their phylogenetic relationships were not resolved within Clade C and they were treated as *O. mamorae* complex (Fig. 1; specimens from southern Bolivia, eastern Paraguay and western Brazil treated as *Oecomys* cf. *mamorae* by Pardiñas *et al.*, 2016). Specimens from northeastern Argentina and western Brazil were recovered as a monophyletic clade (bootstrap = 70% and BPP = 0.96) and are treated as *O. franciscorum* (Fig. 1; specimens from localities 31, 34 and 35 treated as *Oecomys* cf. *franciscorum* by Pardiñas *et al.*, 2016).

Clade D (*O. paricola* species group) was well supported in both ML and BI for single-gene and concatenated data sets (Figs 1, 2; Supporting Information, Fig. S1) and was represented by specimens from the Amazon and northern Cerrado (Fig. 3D). Four highly supported monophyletic clades were recovered in two sister groups (Figs 1, 2): one group from the Cerrado and eastern Amazon (northern and eastern clades), and the other from southern Amazonia (Fig. 3D, western clades). Within the former, one clade comprised specimens from Ilha de Marajó, Pará, Brazil (Figs 1, 3D; locality 55, northern clade) clustered with the clade composed of the remaining specimens from the eastern Amazon and Cerrado (Figs 1, 3D, eastern clade). Two highly supported clades were recovered within the other sister group, the western clades (Figs 1, 3D; specimens from localities 41 and 46).

Clade E (*O. catherinae* species group) was moderately (50/0.78; Fig. 1) to highly supported (94/0.99; Fig. 2) in both ML and BI for the concatenated data set without gaps (Fig. 2) and was composed of specimens from the Atlantic Forest, Cerrado and Amazon biomes (Fig. 3E). Two main groupings were recovered with high node support values: one represented by specimens from the southern Amazon (Fig. 3E, western clade) and its sister clade composed of four distinct monophyletic clades (Figs 1, 2). Specimens from the westernmost clade (locality 58, Figs 1 and 3E, treated as *O. concolor* by Miranda *et al.*, unpublished data and as *Oecomys* cf. *concolor* by Andrades-Miranda *et al.*, 2001) were recovered as the sister group of a clade composed of Atlantic Forest specimens (Figs 1, 3E, eastern clade) and two sister lineages: one from the Cerrado recognized as the central clade [Figs 1, 3E; specimens from localities 22, 24 and 25 treated as *O. concolor* by Miranda *et al.* (unpublished data) and as *Oecomys* cf. *concolor* by Andrades-Miranda *et al.*, 2001] and the other from the eastern Amazon assigned to the northern clade (Figs 1, 3E; specimens from localities 51 and 54

Figure 2. Maximum likelihood (ML) tree using concatenated matrix data set without missing data (Cyt*b* + IRPB + iBF7). Bayesian inference (BI) showed the same topology. Bootstrap and posterior probability support values are above branches for values above 70% and/or above 0.90, respectively. Black bars (on the right of the tree) indicate the species limits as proposed by Bayesian General Mixed Yule Coalescent (bGMYC), Bayesian implementation of Poisson Tree Processes (bPTP), Species Tree Estimation using the maximum likelihood (STEM) and Bayesian Species Delimitation (BSD) analyses. Diploid and fundamental numbers, locality (state: number as cited on the maps) and clades, as indicated in Figure 1.

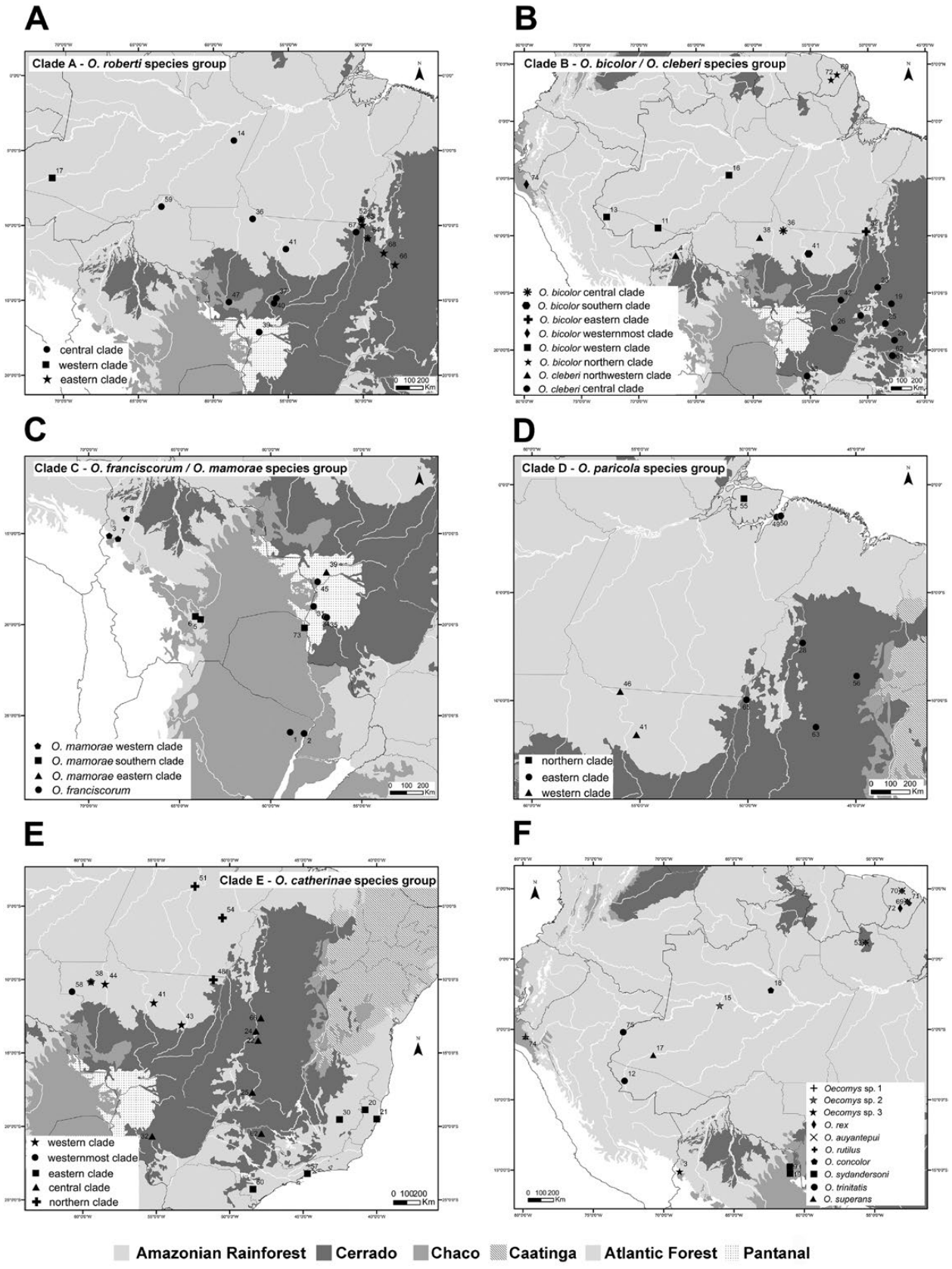

treated as *O. rex* by Pardiñas *et al.* 2016). Discordance between mitochondrial and nuclear gene trees were found within Clade E, with samples from the eastern clade (Fig. 3E) recovered as the sister group of the western clade for nuclear genes reconstruction (bootstrap = 75% and BPP = 0.99) (Supporting Information, Fig. S1, blue branches). These results may explain the lowest support within Clade E for the phylogenetic position of the eastern clade in the concatenated analyses without gaps (Fig. 2; bootstrap = 63.1% and BPP = 0.88).

Coalescent-based species delimitation

The most conserved results among bGMYC and bPTP analyses recognized nine monophyletic lineages as single species (Fig. 1): *O. auyantepui*, *O. concolor*, *O. rex, O. superans, O. sydandersoni, O. trinitatis, Oecomys* sp. 1, *Oecomys* sp. 2 and *Oecomys* sp. 3 (see Figs 1, 3F). In contrast, more than one species was detected within the remaining six lineages, suggesting that *O. bicolor*, *O. catherinae*, *O. cleberi, O. franciscorum*, *O. mamorae*, *O. paricola*, *O. roberti* and *O. rutilus* may represent species complexes (Fig. 1).

Coalescent-based STEM analysis recovered a species tree composed of 17 lineages (Fig. 2) with the highest log-likelihood value (–2786.91751). This analysis detected two species in the *O. roberti* and *O. cleberi* complexes (Clades A and B, respectively), three in the *O. paricola* complex (Clade D), four in the *O. bicolor* complex (Clade B), and five species in the *O. catherinae* complex (Clade E). The lineage represented by the *O. franciscorum* specimens was recovered as a single species (Fig. 2). The topology of the species tree reflects the topology obtained by ML and Bayesian analyses with a concatenated data set without gaps (Fig. 2). BSD analysis was concordant with STEM.

Single-gene (bGMYC and bPTP) and multi-gene (STEM and BSD) species delimitation analyses were concordant in most cases. Yet, bGMYC and bPTP analyses detected two species in *O. franciscorum*, while with the STEM and BSD methods, *O. franciscorum* was considered as a single taxon (Fig. 2). Furthermore, the bPTP analysis recognized the *O. cleberi* complex as one single species, while specimens from Aripuanã, Mato Grosso state, Brazil (Figs 2, 3B; locality 38) were recovered as a different species within Clade B in bGMYC, STEM and BSD analyses (Fig. 2).

Cytogenetics

For Clade A (*O. roberti* species group), two specimens from the central clade (Figs 1, 3A; MZUSP 29526 and M 968464, localities 36 and 41) exhibited $2n = 82$, FN = 106, comprising 27 acrocentric pairs and 13 biarmed pairs with centromeric heterochromatin. The X-chromosome was the largest submetacentric with the short arm heterochromatic and the Y-chromosome was an acrocentric slightly heterochromatic (Fig. 4A). Two additional karyotypes from specimens recovered within Clade A were reported in the literature: $2n = 82$, FN = 110 for a specimen from the central clade (Figs 1, 3A; voucher UFPB 494, locality 59; Andrades-Miranda *et al.*, 2001) and $2n = 80$, FN = 114 for a specimen from the western clade (Figs 1, 3A; voucher JLP15241, locality 17; Patton *et al.*, 2000).

For Clade B (*O. bicolor*/*O. cleberi* species group), specimens recovered in the *O. bicolor* western (Figs 1, 3B; MJJS 68 and MJJS 69, locality 11), central and southern clades (Figs 1, 3B; MZUSP 29523 and MZUSP 29528; localities 36, 41), and one specimen recovered in the *O. cleberi* northwestern clade (Figs 1, 3B; MZUSP 35534, locality 38) shared the same karyotype with $2n = 80$, FN = 140. This karyotype was composed of 31 pairs of metacentric to submetacentric chromosomes and eight pairs of acrocentric chromosomes. The X-chromosome was large and submetacentric with heterochromatic short arm, and the Y-chromosome was an entirely heterochromatic acrocentric (Fig. 4B). One specimen treated as *O. bicolor*, with a similar karyotype of $2n = 80$, FN = 140, was also recovered in the western clade of *O. bicolor* (Figs 1, 3B; MNFS 1499, locality 13; Patton *et al.*, 2000).

Nineteen specimens from the *O. cleberi* central clade (Figs 2, 3B; localities 26, 27, 61 and 62) exhibited karyotypes with $2n = 80$. One individual from Goiás, Brazil and two from São Paulo, Brazil (Figs 2, 3B; localities 27, 61 and 62) exhibited 28 biarmed and 11 acrocentric chromosome pairs (FN = 134) (Fig. 4C). Pericentromeric heterochromatin was evident in all autosomes. The X-chromosome was submetacentric with a heterochromatic short arm and the Y-chromosome was medium-sized acrocentric with an evident heterochromatic block in the distal region of the long arm (Fig. 4C). Five specimens from Goiás, Brazil (Figs 1, 3B; localities 23 and 25) were also recovered in the central clade of *O. cleberi* and exhibited a karyotype with $2n = 80$, FN = 124, which was

Figure 3. Collecting localities of *Oecomys* specimens analysed in this study. Specimen data and locality number as cited in Supporting Information, Table S1. Biome delimitation follows Olson *et al.* (2001). A, Clade A – *O. roberti* species group. B, Clade B – *O. bicolor*/*O. cleberi* species group. C, Clade C – *O. franciscorum*/*O. mamorae* species group. D, Clade D – *O. paricola* species group. E, Clade E – *O. catherinae* species group. F, the remaining ten distinct lineages recovered in molecular analyses based only on sequences downloaded from GenBank (Cyt*b* data set).

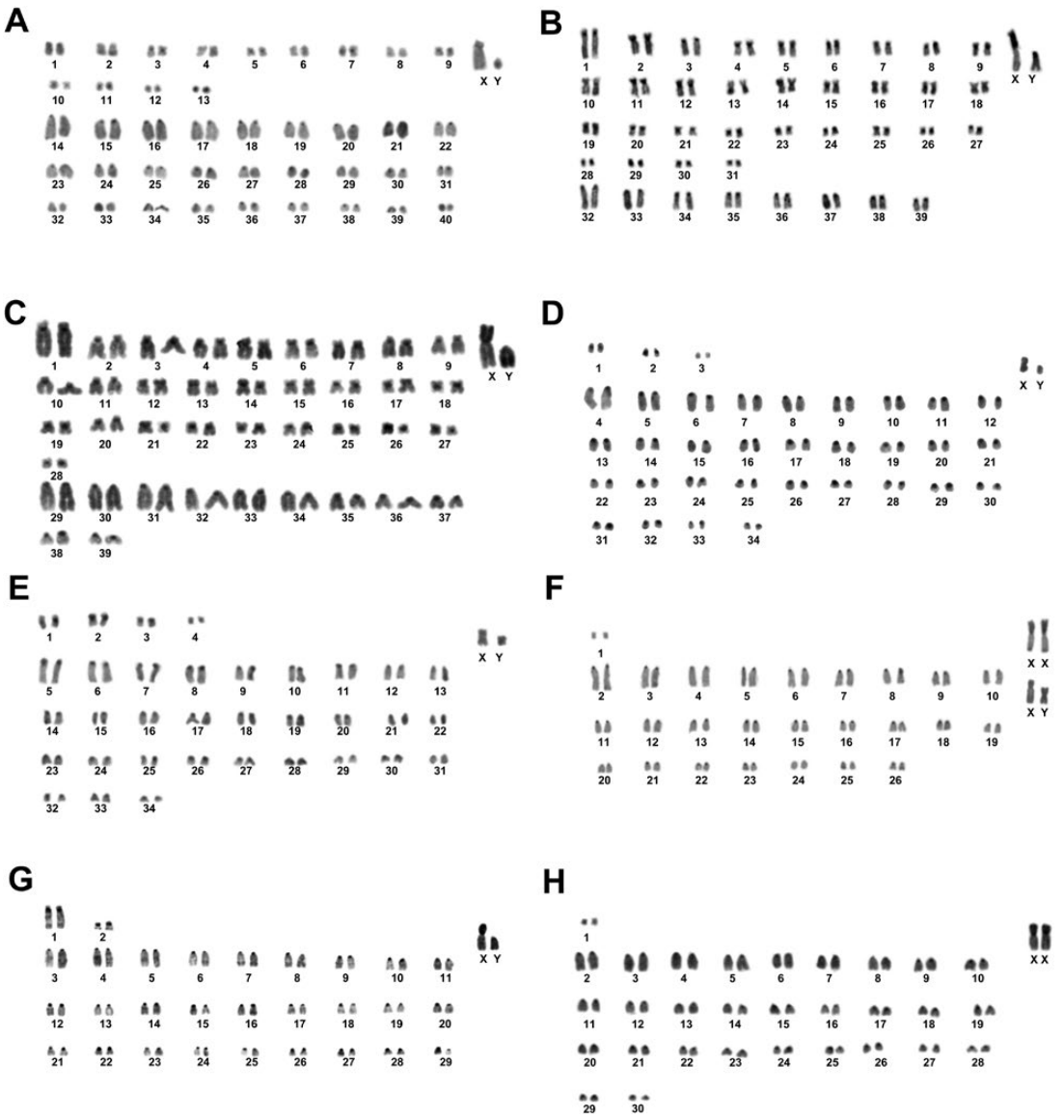

Figure 4. C-banded karyotypes of *Oecomys* specimens. A, $2n$ = 82, FN = 106, of a male specimen MZUSP 29526 from Cláudia, MT (locality 41), treated as *O. roberti* central clade. B, $2n$ = 80, FN = 140, of a male specimen MZUSP 35534 from Aripuanã, MT (locality 38), treated as *O. cleberi* northwestern clade. C, $2n$ = 80, FN = 134, of a male specimen PCH 3617 from São Joaquim da Barra, SP (locality 62), treated as *O. cleberi* central clade. D, $2n$ = 70, FN = 74, of a male specimen MZUSP 29527 from Cláudia, MT (locality 41), treated as *O. paricola* western clade. E, $2n$ = 70, FN = 76, of a male specimen UU 043 from ESEC Uruçuí-Una, PI (locality 56), treated as *O. paricola* eastern clade. F, $2n$ = 54, FN = 54, of a female specimen MZUSP 29516 from Gaúcha do Norte, MT (locality 43), treated as *O. catherinae* western clade. Male sex chromosomes correspond to the specimen MZUSP 35543 from Claudia, MT (locality 62). G, $2n$ = 60, FN = 62, of a male specimen MZUSP 29532 from Aripuanã, MT (locality 38), treated as *O. catherinae* westernmost clade. H, $2n$ = 62, FN = 62, of a female specimen APC 292 from Vila Rica, MT (locality 48), treated as *O. catherinae* northern clade; note submetacentric pair 1 in (G), which is not present in (H) (see text for details); FN, number of autosome arms; MT, Mato Grosso; PI, Piauí; SP, São Paulo.

previously reported by Andrades-Miranda *et al.* (2001) as *Oecomys* cf. *bicolor* cytotype 1.

For Clade C (*O. mamorae*/*O. franciscorum* species group), two *Oecomys* sp. specimens with $2n$ = 72, FN = 90 were reported by Andrade & Bonvicino (2003) and treated as *Oecomys* cf. *franciscorum* by Pardiñas *et al.* (2016) (Figs 1, 3C; LBCE 1924 and LBCE 1941, locality 31). These specimens clustered with others treated by us as *O. franciscorum*.

For Clade D (*O. paricola* species group), the karyotyped specimens recovered in this group exhibited $2n = 70$, except for an individual from Belém, Pará, which showed $2n = 68$, FN = 72 (Figs 1, 3D; locality 50) and was reported by Rosa *et al.* (2012). Additionally, three fundamental numbers associated with distinct clades were found: (1) specimens with $2n = 70$, FN = 72, reported by Rosa *et al.* (2012), were recovered in the northern clade (Figs 1, 3D; locality 55); (2) specimens with $2n = 70$, FN = 76, were recovered within the eastern clade (Figs 1, 3D, 4E; UU 043, locality 56, and those reported by Rosa *et al.* (2012) from locality 50, as well as the specimen with $2n = 68$, FN = 72 previously mentioned); and (3) specimens with $2n = 70$, FN = 74, recovered in the western clade (Figs 3D, 4D; MZUSP 29525 and MZUSP 29527, locality 41). Karyotypes with $2n = 70$, FN = 74 and $2n = 70$, FN = 76 exhibited pericentromeric heterochromatin in all autosomes and had three and five submetacentric pairs, respectively. Both karyotypes showed biarmed sex chromosomes that were slightly heterochromatic, and the X-chromosomes were the largest submetacentrics (Figs 4D, 4E).

For Clade E (*O. catherinae* species group), five specimens recovered in the western clade (Figs 1, 3E; localities 38, 41, 43 and 44) exhibited $2n = 54$, FN = 54 (Fig. 4F). This karyotype is described for the first time in *Oecomys*. All autosomes are acrocentric (pairs 2–26), except for a small submetacentric pair (pair 1). The X-chromosome is large and submetacentric with a short heterochromatic arm, and the Y-chromosome is medium sized, metacentric and entirely heterochromatic (Fig. 4F). These specimens were recovered in the western clade, which is the sister of a lineage composed of four distinct clades (Figs 1, 2, 3E; eastern, central, northern and westernmost clades). Specimens recovered within the eastern (locality 30), westernmost (locality 38) and central clades (locality 62) exhibited identical karyotypes with $2n = 60$, FN = 62 (Fig. 4G). This karyotype is composed of two biarmed pairs and 27 acrocentric pairs. The X-chromosome is large and submetacentric with a short heterochromatic arm, and the Y-chromosome is medium, heterochromatic and acrocentric. One specimen recovered in the westernmost clade (Fig. 1, 3E; MN 37776, locality 58) and 13 specimens recovered in the central clade (Figs 1, 3E; localities 22, 24 and 25), reported by Andrades-Miranda *et al.* (2001) as *Oecomys* cf. *concolor*, also showed a karyotype with $2n = 60$, FN = 62 (Fig. 1). Six females from the northern clade (Figs 1, 2, 3E; locality 48) had a novel karyotype for the genus, with $2n = 62$, FN = 62, which was composed of one small biarmed pair (pair 1) and 29 acrocentric pairs (pairs 2–30). The X-chromosome is large and submetacentric with a block of heterochromatin in the short arm (Fig. 4H).

Cytogenetic information is also available for other specimens with sequences obtained from GenBank (Patton *et al.*, 2000): (i) those treated as *O. superans* from Penedo, Amazonas, Brazil (Fig. 3F, locality 17) with $2n = 80$, FN = 108, recovered in a monophyletic lineage together with other specimens from Peru (Figs 1, 3F; locality 74); (ii) specimens treated as *O. trinitatis* from Igarapé Porangaba, Acre, Brazil (Fig. 3F, locality 12) with $2n = 58$, FN = 96, also recovered in a monophyletic lineage together with other specimens from Peru (Figs 1, 3F; locality 75); (iii) and one specimen treated as *Oecomys* sp. 2 (Fig. 3F, locality 15), with $2n = 86$, FN = 98 (Fig. 1).

Morphologic analyses

Specimens recovered in the five major clades (A–E) and specimens within each of these clades (Figs 1, 2) differed consistently in the qualitative characters of their external morphology (dorsal and ventral pelage coloration, tail coloration and tuft development), skull morphology (shape of incisive foramina, presence of alisphenoid strut, size of subsquamosal fenestra, carotid and stapedial circulatory pattern, and the interorbital region morphology, including shape and development of supraorbital margins and temporal ridges) and general size. The results of these morphological comparisons are summarized in Tables 2 and 3 and Supporting Information, Table S3.

For Clade A (*O. roberti* species group), specimens from the central clade (Fig. 3A; $n = 7$; see Appendix II) exhibited intermediate size (CIL: 27.90–28.70 mm; LM: 4.50–4.90 mm; Table 2); moderately long pelage with a well-delimited distinction between dorsal (tawny brown, somewhat orangish) and ventral (self-coloured white) pelage coloration; and a brown, unicoloured tail without a terminal apical tuft. Skull characterized by a mid-sized rostrum; interorbital region convergent anteriorly, with moderately developed supraorbital margins and temporal ridges; short incisive foramen (distant from M1 level), and tear drop shaped; anterior margin of the mesopterygoid fossa generally U-shaped, and sphenopalatine vacuities absent (mesopterygoid roof completely ossified); palate long and wide (mesopterygoid fossa never reaches M3 level), postero-lateral palatal pits frequently large; carotid and stapedial circulatory pattern 1 (*sensu* Voss, 1988); alisphenoid strut absent, and hamular process of squamosal narrow and not occluding the subsquamosal fenestra, except in the individual MZUSP 35547 (see Table 3).

Clade B (*O. bicolor*/*O. cleberi* species group) contained the smallest specimens in our sample. Two morphologies were recognized that do not overlap in size measurements. Although their qualitative characters are somewhat similar, side-by-side comparisons successfully distinguished specimens treated as the *O.*

Table 2. Descriptive statistics of external and craniodental measurements (in millimetre) and weight (in grams) of adult *Oecomys* specimens analysed in this study

	Clade	A	B		C	D		E				
	Lineages	*O. roberti* central clade	*O. bicolor* southern clade	*O. cleberi* central clade	*O. franciscorum*	*O. paricola* western clade	*O. paricola* eastern clade	*O. catherinae* eastern clade	*O. catherinae* western clade	*O. catherinae* westernmost clade	*O. catherinae* central clade	*O. catherinae* northern clade
	General size	Medium	Small	Small	Large	Medium	Medium	Large	Large	Large	Large	Large
HBL	Mean ± SD	120.3 ± 2.9	89.3 ± 4.0	–	139.3 ± 7.9	–	112.5 ± 8.7	129.4 ± 7.3	–	–	–	122.9 ± 8.2
	Range (*N*)	117–122 (3)	85–93 (3)	107–119 (2)	129–146 (4)	120–122 (2)	98–123 (6)	123–140 (5)	130 (1)	125–140 (2)	112 (1)	109–130 (5)
TL	Mean ± SD	141.7 ± 15.0	–	–	167.0 ± 10.5	–	129.0 ± 9.9	173.8 ± 8.3	–	–	–	143.6 ± 8.8
	Range (*N*)	133–159 (3)	76–100 (2)	117–118 (2)	158–180 (4)	128–130 (2)	115–137 (6)	167–185 (4)	139 (1)	155–161 (2)	147 (1)	133–154 (5)
HFL	Mean ± SD	26.7 ± 1.5	21.3 ± 0.3	–	30.3 ± 1.2	–	24.5 ± 2.2	30.0 ± 2.1	–	–	–	26.9 ± 0.2
	Range (*N*)	25–28 (3)	21.0–21.5 (3)	22–22 (2)	29–32 (4)	19.5–25.0 (2)	22–27 (6)	27–33 (5)	26 (1)	29–29 (2)	26 (1)	26.5–27.0 (5)
W	Mean ± SD	53.5 ± 12.7	24.8 ± 4.4	–	79.0 ± 15.8	–	55.2 ± 10.9	65.0 ± 14.0	–	–	–	60.2 ± 9.0
	Range (*N*)	40.6–66.0 (3)	20.0–28.5 (3)	36–47 (2)	60–94 (4)	53–54 (2)	45–71 (6)	52–89 (5)	55 (1)	72–80 (2)	–	46–71 (5)
CIL	Mean ± SD	28.4 ± 0.3	23.5 ± 1.0	26.2 ± 0.6	30.4 ± 1.5	27.7 ± 1.0	27.4 ± 1.0	31.5 ± 1.3	–	–	29.6 ± 1.0	28.4 ± 0.5
	Range (*N*)	27.9–28.7 (4)	22.5–24.5 (3)	25.2–26.7 (6)	28.2–32.3 (5)	26.5–28.5 (3)	25.8–28.3 (6)	29.3–32.9 (5)	29.5 (1)	29.5–30.5 (2)	28.8–30.8 (3)	27.6–29.0 (5)
LD	Mean ± SD	7.8 ± 0.0	6.5 ± 0.4	7.4 ± 0.1	8.4 ± 0.6	7.8 ± 0.5	7.9 ± 0.3	8.7 ± 0.3	–	–	7.9 ± 0.5	7.8 ± 0.2
	Range (*N*)	7.7–7.9 (4)	6.2–6.9 (3)	7.2–7.6 (6)	7.3–9.0 (5)	7.2–8.2 (3)	7.4–8.4 (6)	8.2–9.0 (5)	7.9 (1)	7.9–8.3 (2)	7.4–8.4 (3)	7.4–7.9 (5)
LM	Mean ± SD	4.7 ± 0.2	3.6 ± 0.0	4.1 ± 0.0	5.1 ± 0.2	4.7 ± 0.4	4.2 ± 0.1	5.3 ± 0.2	–	–	5.1 ± 0.2	5.0 ± 0.2
	Range (*N*)	4.5–4.9 (4)	3.5–3.6 (3)	4.0–4.2 (6)	4.9–5.4 (5)	4.2–5.0 (3)	4.0–4.3 (6)	5.0–5.5 (5)	5.2 (1)	5.2–5.8 (2)	4.9–5.3 (3)	4.8–5.2 (5)
BM1	Mean ± SD	1.3 ± 0.1	1.0 ± 0.0	1.2 ± 0.0	1.5 ± 0.0	1.3 ± 0.0	1.2 ± 0.0	1.5 ± 0.6	–	–	1.4 ± 0.0	1.4 ± 0.2
	Range (*N*)	1.2–1.4 (4)	0.9–1.0 (3)	1.2–1.3 (6)	1.4–1.5 (5)	1.2–1.3 (3)	1.2–1.3 (6)	1.4–1.5 (5)	1.4 (1)	1.5–1.6 (2)	1.4–1.5 (3)	1.3–1.6 (5)
LIF	Mean ± SD	5.2 ± 0.3	4.4 ± 0.2	5.2 ± 0.2	6.3 ± 0.5	5.0 ± 0.5	5.1 ± 0.3	5.7 ± .03	–	–	5.6 ± 0.2	5.4 ± 0.2
	Range (*N*)	4.8–5.5 (4)	4.1–4.5 (3)	4.9–5.4 (6)	5.5–6.9 (5)	4.5–5.6 (3)	4.7–5.4 (6)	5.2–6.0 (5)	5.6 (1)	4.9–5.4 (2)	5.4–5.8 (3)	5.2–5.6 (5)
BIF	Mean ± SD	2.7 ± 0.1	2.0 ± 0.1	2.4 ± 0.0	3.0 ± 0.2	2.6 ± 0.0	2.5 ± 0.1	2.8 ± 0.2	–	–	2.5 ± 0.1	2.5 ± 0.1
	Range (*N*)	2.6–2.8 (4)	1.9–2.1 (3)	2.4–2.6 (6)	2.7–3.2 (5)	2.5–2.6 (3)	2.4–2.6 (6)	2.5–3.0 (5)	2.7 (1)	2.4–2.5 (2)	2.4–2.6 (3)	2.4–2.6 (5)
BPB	Mean ± SD	3.1 ± 0.2	2.7 ± 0.2	3.0 ± 0.1	3.3 ± 0.3	3.1 ± 0.1	3.0 ± 0.0	3.1 ± 0.1	–	–	3.3 ± 0.2	3 .0 ± 0.2
	Range (*N*)	2.9–3.3 (4)	2.5–2.9 (3)	2.8–3.3 (6)	3.0–3.6 (5)	3.0–3.3 (3)	3.0–3.1 (6)	3.0–3.1 (5)	3.5 (1)	3.1–3.3 (2)	3.0–3.4 (3)	2.7–3.3 (5)
BZP	Mean ± SD	3.0 ± 0.1	2.3 ± 0.1	2.6 ± 0.1	3.7 ± 0.3	2.6 ± 0.1	2.8 ± 0.1	3.8 ± 0.2	–	–	3.6 ± 0.1	3.7 ± 0.2
	Range (*N*)	2.8–3.1 (4)	2.2–2.4 (3)	2.5–2.7 (6)	3.2–4.0 (5)	2.5–2.7 (3)	2.6–2.9 (6)	3.6–4.0 (5)	3.6 (1)	3.1–3.5 (2)	3.4–3.7 (3)	3.3–4.0 (5)
LR	Mean ± SD	9.1 ± 0.2	7.1 ± 0.3	8.3 ± 0.3	9.8 ± 0.4	8.7 ± 0.0	8.6 ± 0.3	10.6 ± 0.2	–	–	9.9 ± 0.8	9.5 ± 0.3
	Range (*N*)	8.8–9.4 (4)	6.9–7.5 (3)	7.7–8.7 (6)	9.3–10.2 (5)	8.7–8.8 (3)	8.0–8.9 (6)	10.2–10.8 (5)	10.0 (1)	10.0–10.3 (2)	9.4–10.8 (3)	9.1–9.9 (5)
LN	Mean ± SD	10.7 ± 0.2	8.4 ± 0.8	9.4 ± 0.3	11.1 ± 0.5	10.0 ± 0.3	10.1 ± 0.5	11.5 ± 0.6	–	–	10.5 ± 0.3	12.4 ± 3.9
	Range (*N*)	10.4–10.9 (4)	7.7–9.1 (3)	9.0–9.9 (6)	10.5–11.7 (5)	9.8–10.3 (3)	9.5–10.7 (6)	10.8–12.2 (5)	11.1 (1)	10.3–11.4 (2)	10.2–10.8 (3)	10.3–19.4 (5)
LIB	Mean ± SD	5.6 ± 0.1	4.5 ± 0.1	5.1 ± 0.1	5.3 ± 0.3	5.5 ± 0.2	5.2 ± 0.3	6.1 ± 0.3	–	–	5.7 ± 0.4	5.5 ± 0.3
	Range (*N*)	5.4–5.6 (4)	4.4–4.6 (3)	4.9–5.3 (6)	4.9–5.7 (5)	5.2–5.6 (3)	4.7–5.5 (6)	5.6–6.3 (5)	5.2 (1)	5.7–5.8 (2)	5.3–6.1 (3)	5.1–5.9 (5)
BB	Mean ± SD	13.4 ± 0.3	11.8 ± 0.1	12.9 ± 0.4	13.6 ± 0.1	13.12 ± 0.33	12.7 ± 0.4	14.4 ± 0.9	–	–	13.5 ± 0.0	–
	Range (*N*)	13.0–13.7 (4)	11.7–11.9 (3)	12.4–13.4 (6)	13.4–13.7 (5)	12.9–13.5 (3)	12.3–13.3 (6)	12.8–15.1 (5)	13.4 (1)	13.1–13.2 (2)	13.5–13.6 (3)	12.8–13.3 (5)

Table 2. *Continued*

	Clade	A	B		C	D		E				
	Lineages	*O. roberti* central clade	*O. bicolor* southern clade	*O. cleberi* central clade	*O. franciscorum*	*O. paricola* western clade	*O. paricola* eastern clade	*O. catherinae* eastern clade	*O. catherinae* western clade	*O. catherinae* westernmost clade	*O. catherinae* central clade	*O. catherinae* northern clade
	General size	Medium	Small	Small	Large	Medium	Medium	Large	Large	Large	Large	Large
ZB	Mean ± SD	16.6 ± 0.2	14.2 ± 0.5	15.3 ± 0.4	17.7 ± 1.0	16.5 ± 0.7	15.9 ± 0.7	17.7 ± 1.0	–	–	16.5 ± 0.7	16.1 ± 0.7
	Range (*N*)	16.3–16.7 (4)	13.7–14.8 (3)	14.6–15.7 (6)	16.5–19.0 (5)	15.9–17.3 (3)	15.1–16.9 (6)	16.1–19.0 (5)	17.1 (1)	16.4–16.8 (2)	15.8–17.3 (3)	15.3–17.1 (5)
ZL	Mean ± SD	14.2 ± 0.2	11.6 ± 0.3	12.7 ± 0.3	15.3 ± 1.0	13.56 ± 0.6	13.7 ± 0.3	–	–	–	14.7 ± 0.4	14.2 ± 0.8
	Range (*N*)	13.9–14.5 (4)	11.3–11.9 (3)	12.4–13.2 (6)	13.8–16.4 (5)	12.9–14.1 (3)	13.3–14.1 (6)	–	14.3 (1)	14.8–15.4 (2)	14.4–15.2 (3)	13.3–15.3 (5)

Mean values given for variables with more than two specimens examined.
BB, breadth of the braincase; BIF, breadth of the incisive foramina; BM1, breadth of first upper molar; BPB, breadth of the palatal bridge; BZP, breadth of the zygomatic plate; CIL, condyle-incisive length; HBL, head and body length; HFL, hindfoot length including claw; LD, length of the diastema; LIB, interorbital breadth; LIF, length of the incisive foramina; LM, crown length of the upper molar series; LN, length of nasals; LR, length of the rostrum; *N*, number of specimens; TL, tail length; W, body mass; ZB, breadth across the squamosal zygomatic processes; ZL, zygomatic length.

bicolor complex from the *O. cleberi*. *Oecomys bicolor* complex (Fig. 3B; central and southern clades, $n = 5$; see Appendix II) is represented by the smallest specimens (CIL: 22.50–24.50 mm; LM: 3.50–3.60 mm; Table 2). Individuals have short pelage with well-delimited distinction between dorsal (rufous orange brown) and ventral (self-coloured white) pelage coloration, and a brown, unicoloured tail with a poorly developed apical tuft. The skull is characterized by a relatively short rostrum; interorbital region anteriorly convergent with poorly developed supraorbital margins (temporal ridges absent); incisive foramen long (close to M1 level), narrow and oval in shape; anterior margin of the mesopterygoid fossa U-shaped; sphenopalatine vacuities absent (mesopterygoid roof completely ossified); palate long and wide (mesopterygoid fossa never reaches M3 level) with small postero-lateral palatal pits; carotid and stapedial circulatory pattern 1 (*sensu* Voss, 1988); alisphenoid strut absent (except in MZUSP 29528); and hamular process of the squamosal narrow and not occluding the subsquamosal fenestra (see Table 3). In the *O. cleberi* complex (Fig. 3B; central and northwestern clades, $n = 9$; see Appendix II), specimens from central clade ($n = 7$) are small (CIL: 25.20–26.70 mm; LM: 4.00–4.20 mm; Table 2), but larger than those from *O. bicolor* central and southern clades and *O. cleberi* northwestern clade. Pelage is intermediate in length with a well-delimited distinction between dorsal (yellowish orange brown) and ventral (self-coloured white) coloration; tail brown, unicoloured or weakly bicoloured, with a poorly developed apical tuft. Skull with a relatively short rostrum; interorbital region convergent anteriorly with poorly developed supraorbital margins (temporal ridges absent); incisive foramen long (close to M1 level) and oval in shape; anterior margin of the mesopterygoid fossa U-shaped; sphenopalatine vacuities absent (mesopterygoid roof totally ossified); palate long and wide (mesopterygoid fossa never reaches M3 level); postero-lateral palatal pits notably small; carotid and stapedial circulatory pattern 1 (*sensu* Voss, 1988); alisphenoid strut usually absent and buccinator-masticatory and foramen ovale confluent and distinctly large; hamular process of the squamosal narrow and not occluding the subsquamosal fenestra (see Table 3). *Oecomys cleberi* specimens from the northwestern clade are morphologically similar to *O. bicolor* specimens from the central and southern clades. Therefore, characters of *O. cleberi* from the northwestern clade are summarized in Table 3 within the *O. bicolor* lineages. These two morphologies (one corresponding to the central and southern clades of *O. bicolor* and the northwestern clade of *O. cleberi* and the other to specimens from the central clade of *O. cleberi*) have similar qualitative external and craniodental characters. They can be distinguished mainly by overall size, dorsal pelage length and colouration (Tables 2, 3). However, central

Table 3. Qualitative external and craniodental morphological characters of *Oecomys* specimens analysed in this study

Clade	A	B		C	D		E				
	O. roberti central clade (n = 7)	*O. bicolor* central/ southern clade (n = 5)	*O. cleberi* central clade (n = 7)	*O. franciscorum* (n = 5)	*O. paricola* western clade (n = 9)	*O. paricola* eastern clade (n = 6)	*O. catherinae* western clade (n = 5)	*O. catherinae* eastern clade (n = 7)	*O. catherinae* westernmost clade (n = 3)	*O. catherinae* central clade (n = 4)	*O. catherinae* northern clade (n = 8)
Dorsal pelage	Tawny brown (intermediate)	Rufous orange brown (short)	Yellowish orange brown (intermediate)	Greyish brown (intermediate), with orangish mystacial and ear regions	Tawny brown (inter mediate)	Dark ochraceous brown (inter mediate)	Tawny brown (long and relatively lax)	Ochraceous brown (long and distinctively lax)	Tawny chestnut (long and lax)	Tawny brown to brown (long)	Tawny chestnut (long and relatively lax)
Ventral pelage	Self-coloured white	Self-coloured white	Self-coloured white	Self-coloured dull white/ yellowish	Grey-based and white tipped*	Grey-based and white tipped*	Grey-based and white tipped	Grey-based and white tipped**	Grey-based and white tipped*	Grey-based and white tipped***	Grey-based and white tipped*
Tail	Brown (unicoloured)	Brown (unicoloured)	Brown (unicoloured weakly bicoloured)	Brown (weakly bicoloured)	Brown to dark brown (unicoloured)	Dark brown (unicoloured)	Brown (weakly bicoloured)	Brown (weakly bicoloured)	Dark brown (unicoloured)	Brown (weakly bicoloured)	Brown (weakly bicoloured)
Tail tuft	Absent	Poorly developed	Poorly developed	Absent to poorly developed	Developed	Developed	Absent to poorly developed	Poorly developed	Absent to poorly developed	Poorly developed	Poorly developed
Incisive foramina****	Short and tear drop shaped	Long, narrow and oval	Long and oval	Long and oval	Short, narrow and oval*****	Short, tear drop shaped	Long and oval	Short and oval	Short and oval	Long and oval	Short and oval
Interorbital region	Convergent	Convergent	Convergent	Weakly convergent	Convergent	Convergent	Convergent	Strongly convergent	Strongly convergent	Strongly convergent	Strongly convergent
Supraorbital margins and temporal ridges	Moderately developed	Poorly developed	Poorly developed	Moderately developed	Moderately developed	Developed	Developed	Highly developed	Highly developed	Highly developed	Highly developed
Alisphenoid strut	Absent	Usually absent	Absent	Usually absent	Absent	Absent	Absent	Usually absent	Usually absent	Absent	Usually absent

Table 3. *Continued*

Clade	A	B		C	D		E				
	O. roberti central clade (n = 7)	*O. bicolor* central/ southern clade (n = 5)	*O. cleberi* central clade (n = 7)	*O. franciscorum* (n = 5)	*O. paricola* western clade (n = 9)	*O. paricola* eastern clade (n = 6)	*O. catherinae* western clade (n = 5)	*O. catherinae* eastern clade (n = 7)	*O. catherinae* westernmost clade (n = 3)	*O. catherinae* central clade (n = 4)	*O. catherinae* northern clade (n = 8)
Subsquamosal foramen	Present	Present	Present	Present (Usually large)	Present (occluded by hamular process)	Present (not occluded by hamular process)	Usually small	Usually small	Usually small	Usually occluded by hamular process	Usually absent
Circulatory pattern	1	1	1	3	1	1	1	1	1	1	1

*Except chin and neck (self-coloured white).
**With orange wash (below chest) and self-coloured white (above chest).
***Except Tocantins state specimens: self-coloured white.
****Except Tocantins state specimens: self-coloured white.
*****Specimens from Piauí state exhibited only oval.

clade specimens of *O. cleberi* have smaller postero-lateral palatal pits and a larger buccinator-masticatory/foramen ovale confluence, when compared to the other specimens from the Amazon biome.

For Clade C (*O. mamorae*/*O. franciscorum* species group), specimens treated as *O. franciscorum* (Fig. 3C, n = 5; see Appendix II) exhibited large size (CIL: 28.20–32.30 mm; LM: 4.90–5.40 mm) and the largest mean (CIL: 30.36 mm) (Table 2). Pelage moderately long, with a well-delimited distinction between dorsal (greyish brown, ochraceous) and ventral (self-coloured dull white/yellowish) pelage colouration; mystacial region slightly orange (ochre or reddish); tail brown and weakly bicoloured with a poorly developed or absent apical tuft. Skull characterized by a mid-sized rostrum, and interorbital region weakly convergent anteriorly with moderately developed supraorbital margins and temporal ridges; incisive foramen distinctively long (close to M1 level) and oval shaped; anterior margin of the mesopterygoid fossa U-shaped; sphenopalatine vacuities absent (mesopterygoid roof totally ossified); palate long and wide (mesopterygoid fossa never reaches M3 level) with frequently large postero-lateral palatal pits; carotid and stapedial circulatory pattern 3 (*sensu* Voss, 1988), alisphenoid strut usually absent; hamular process of the squamosal never occludes the subsquamosal fenestra, which is distinctively large when compared to other *Oecomys* specimens (Table 3).

For Clade D (*O. paricola* species group), specimens treated as *O. paricola* complex (Fig. 3D; eastern and western clades, n = 15; see Appendix II) exhibited intermediate size (eastern clade: CIL: 25.80–28.30 mm; LM: 4.00–4.30 mm; western clade: CIL: 26.50–28.50 mm; LM: 4.20–5.00 mm; Table 2) and moderately long pelage with a well-delimited distinction between dorsal (tawny brown to ochraceous brown) and ventral (grey-based hairs, except for the self-coloured white chin and neck) pelage coloration; tail brown/dark brown and unicoloured with a developed apical tuft. Skull characterized by a relatively short rostrum, interorbital region convergent anteriorly with developed to moderately developed supraorbital margins and temporal ridges; incisive foramen highly variable in shape, exhibiting teardrop (eastern clade specimens), oval or narrow shapes (western clade specimens), but all short (distant from M1 level); anterior margin of the mesopterygoid fossa U-shaped, sphenopalatine vacuities frequently absent (mesopterygoid roof completely ossified); palate long and wide (mesopterygoid fossa never reaches M3 level) with postero-lateral palatal pits frequently small; carotid and stapedial circulatory pattern 1 (*sensu* Voss, 1988); alisphenoid strut absent, and the hamular process of squamosal occludes the subsquamosal fenestra in western clade specimens, but never in specimens from the eastern clade (see

Table 3). Regardless of the morphological similarity between specimens from the eastern and western clades in some traits, we can distinguish these two groups by craniodental measurements (larger in the western clade specimens), dorsal and ventral pelage coloration (darker in the western clade specimens), and morphology of the incisive foramen and subsquamosal fenestra (see Tables 2, 3).

For Clade E (*O. catherinae* species group), large size, grey-based hairs in ventral pelage coloration (grizzled venter) and broad molars (BM1 > 1.40 mm) characterize the morphologically similar lineages within this clade (Tables 2, 3). These specimens contrast with samples from Clades A, B and C, which have self-coloured hairs in the ventral pelage (pure white or yellowish venter) and smaller size, except for Clade C, which has the largest specimens within the samples examined. Only one adult specimen was available for morphometric analyses from the western clade (MZUSP 35537), but qualitative characters from young specimens (Fig. 3E; western clade, n = 4; see Appendix II) were analysed. Adult specimen large (CIL: 29.50 mm; LM: 5.20 mm; Table 2); pelage long, dense and relatively lax, with a poorly delimited distinction between dorsal (tawny brown) and ventral (grey-based and white tipped hairs) pelage colouration; tail brown and unicoloured in juveniles and weakly bicoloured in the adult, with a poorly developed or no apical tuft. Skull characterized by a moderately long and broad rostrum; interorbital region convergent anteriorly, with developed supraorbital margins and temporal ridges; incisive foramen long (close to M1 level) and oval shaped; anterior margin of the mesopterygoid fossa U-shaped; sphenopalatine vacuities absent (mesopterygoid roof completely ossified); palate long and wide (mesopterygoid fossa never reaches M3 level), with distinctively large postero-lateral palatal pits; carotid and stapedial circulatory pattern 1 (*sensu* Voss, 1988); alisphenoid strut absent, and hamular process of squamosal wide and never occluding the subsquamosal fenestra, which is present as a small fenestra in most specimens (Table 3). Specimens from eastern, central, northern and westernmost clades (Fig. 3E) were also large (CIL mean > 28.42 mm; LM mean > 5.00 mm; Table 2). These specimens also share long, dense and soft pelage (especially those from the westernmost clade), with poorly delimited distinction between dorsal (from ochraceous to chestnut, and tawny brown) and ventral (grey-based and white tipped hairs) pelage colouration, except for the self-coloured white specimens from Paranã, Tocantins (locality 66; central clade in Fig. 3E); tail brown and weakly bicoloured (except for the brown unicoloured tail in westernmost clade specimens); self-coloured patches of white hairs in the gular/pectoral region; and interorbital region with highly developed supraorbital margins and temporal ridges; presence of palatal excrescences (poorly to highly developed), not observed in specimens from western clade. Another distinctive difference between specimens from these clades and other lineages (Clades A–D) is the presence of a small postorbital ridge located at the frontosquamosal suture (Table 3). Skull characterized by a moderately long and broad rostrum, incisive foramen moderately short (not reaching the M1 level) and oval shaped; anterior margin of the mesopterygoid fossa U-shaped; sphenopalatine vacuities absent; palate long and wide (mesopterygoid fossa never reaches M3 level), with distinctively large postero-lateral palatal pits; carotid and stapedial circulatory pattern 1 (*sensu* Voss, 1988); alisphenoid strut absent; hamular process of squamosal generally not occluding the subsquamosal fenestra (except in specimens from central clade), which is present as a distinctively small fenestra (Table 3). Side-by-side comparisons allowed for distinction between specimens from each monophyletic lineage within this clade, mainly through morphological external characters. The most informative are the tail length and coloration, the dorsal and ventral pelage coloration, and the texture of the pelage (Table 3). The most conspicuous craniodental differences were a subsquamosal fenestra occluded by the hamular process in the central clade specimens (versus absence in the northern clade or not occluded in the other clades), conspicuously larger molars in specimens from the westernmost clade (Tables 2, 3) and the length of incisive foramen which is moderately short in specimens from the westernmost, northern and eastern clades, and long and close to M1 level in specimens from the central clade (Table 3).

DISCUSSION

Phylogenetic relationships within *Oecomys*

Our analysis represents the most inclusive study of *Oecomys* phylogeny to date, as it includes 14 representatives out of the 17 currently recognized taxa (only *O. flavicans*, *O. phaeotis* and *O. speciosus* were not represented), reinforcing the validity of these taxonomic entities (see Carleton & Musser, 2015) as distinct and monophyletic lineages. Additionally, this is the first study to infer robust phylogenetic relationships among *O. roberti*, *O. franciscorum*, *O. bicolor*, *O. cleberi*, *O. paricola* and *O. catherinae*.

Major lineages were concordant when single and multi-locus data sets were assayed. Nevertheless, multilocus analyses showed robust phylogenetic relationships among lineages despite their less inclusive data set. Species delimitations using bGMYC and bPTP (single-locus) were congruent with STEM and BSD analyses (multi-locus) in the majority of cases. These analyses are complementary validation approaches that

use different strategies to simplify the parameter space of species delimitation (Carstens *et al.*, 2013). Despite the robustness of the multi-locus analyses, the concatenated multi-gene data set with missing data (topology similar to the single-gene, Cyt*b* data set) did not recover the same resolution of analyses as without missing data, probably due to the effect of gaps in the phylogenetic reconstruction. Moreover, the performance of multi-locus analyses with a large percentage of missing data for species delimitation has not been thoroughly investigated (Kubatko *et al.*, 2009; Carstens & Dewey, 2010). Therefore, we decided to use single and multi-locus analyses together (Figs 1, 2). The phylogenetic relationships we recovered were consistent with the results of several other phylogenetic studies based on molecular sequences. For instance, the close phylogenetic relationship between *O. roberti* (central and western clades) and *Oecomys* gr. *roberti* (eastern clade) represented in Clade A (Rocha *et al.*, 2015), the *O. bicolor* and *O. cleberi* affinities recovered in Clade B (Rocha *et al.*, 2012) and the monophyletic group composed of *O. franciscorum* and *O. mamorae* represented in Clade C (Rocha et al., 2012, 2015; Pardiñas *et al.*, 2016).

Species and species group limits: combined analyses on phylogeny, karyology and morphology

We recognized as valid species or species groups those recovered as distinct lineages and/or species in the molecular analyses, and those that can be diagnosed with another approach used in this study, such as morphology or karyology, as well as their geographic distribution.

Following these assumptions, we treated *O. rex*, *O. auyantepui*, *O. rutilus*, *O. concolor*, *O. sydandersoni*, *O. trinitatis* and *O. superans* as valid and distinct taxa in *Oecomys*, which is in accordance with previous authors who used morphology, karyotype and distribution to delimit these taxa (Patton & Da Silva, 1995; D'Elía, 2003; Weksler, 2003; Percequillo *et al.*, 2011; Rocha *et al.*, 2011; Rosa *et al.*, 2012; Carleton & Musser, 2015; Pardiñas *et al.*, 2016). A specimen (MVZ 155005), first treated as *O. concolor* by Weksler (2003, 2006) and subsequently assigned to *O. roberti* by Carleton *et al.* (2009), was treated as a distinct species in this study (*Oecomys* sp. 1), since it was recovered as a distinct and highly divergent lineage (Cyt*b* K2P distance from 6.2 to 14.1% and as one species in single-locus delimitation analyses) and it was neither related to samples of *O. roberti* nor *O. concolor*. Additionally, two undescribed taxa recovered as highly divergent monophyletic lineages were also not related to any species or species group (*Oecomys* sp. 2 and *Oecomys* sp. 3, Cyt*b* K2P from 5.5 to 12.5%), and were already treated as distinct species under the genus: '*Oecomys* sp.' from Lago Vai-Quem-Quer, Amazonas, Brazil (Patton *et al.*, 2000) and '*Oecomys* sp.' from Yucumo, Beni, Bolivia (Pardiñas *et al.*, 2016).

The other delimited taxa were recovered as part of five species groups (Clades A–E). Taking into account coalescent-based species delimitation analyses, we found at least 18 distinct species proposed by bGMYC analyses and 17 species by bPTP, STEM and BSD analyses (Fig. 2). Recently, these coalescent analyses have been associated with an overestimation of species numbers, probably related to the statistical inability of coalescent methods to discriminate between population structure and isolation with species boundaries (Sukumaran & Knowles, 2017). Our conservative hypothesis is that these samples are structured in five species groups containing 15 species as follows:

Oecomys roberti species group (Clade A) – composed of three distinct clades:

(i) *O. roberti* central clade: represented by specimens distributed throughout Pantanal, northwestern Cerrado and southern/central Amazon, and karyotypes with 2*n* = 82, FN = 106 and 110. The sample studied includes specimens close to the type locality of *O. roberti*, Chapada dos Guimarães, Mato Grosso, Brazil, and very likely represent topotypes (APM 890 and MZUSP 35547 from APM Manso, Chapada dos Guimarães). Moreover, morphological characters were similar to those described for specimens from the type locality (Rocha *et al.*, 2011), and those treated as *O. roberti* by other authors (e.g. Patton *et al.*, 2000; Carleton *et al.*, 2009). Thus, the proper taxon name for specimens recovered in the central clade would be *O. roberti* (Thomas, 1904). One specimen from southwestern Amazon, Rondônia State, Brazil (UFPB 494), recovered as a distinct species in coalescent-based delimitation methods, was the most divergent specimen (Cyt*b* K2P: 2.3–3.3%) within the central clade and exhibited a distinct karyotype (2*n* = 82, FN = 110; Andrades-Miranda *et al.*, 2001). Since we did not examine the morphology of this specimen, we regard these differences as intraspecific variation based on the molecular results. Another specimen from Rondônia, Brazil, which was not included in the molecular analyses, had a karyotype similar to other specimens from the central clade (2*n* = 82, FN = 106) and was treated as *O. roberti* (see Langguth *et al.*, 2005). This reinforces that cytogenetic data can be used as a diagnostic trait in this group, as occurs in other taxa of sigmodontine rodents (Paresque *et al.*, 2007; Pereira & Geise, 2007; Geise *et al.*, 2010; Di-Nizo *et al.*, 2014).

(ii) *Oecomys roberti* eastern clade: represented by specimens from northern Cerrado with high genetic divergence (Cyt*b* K2P: 5.2–9.1% compared to central and western clades). Although these specimens were not morphologically examined

and cytogenetic data are absent, they were recognized as a distinct species by both coalescent-based delimitation methods. They were detected in sympatry with specimens from the central clade and had already been treated as a distinct lineage from typical *O. roberti* specimens (Rocha *et al.*, 2011, 2012, 2014, 2015).

(iii) *Oecomys roberti* western clade: represented by one specimen from the western Amazon (JLP 15241) that exhibits a distinct karyotype in relation to the central clade ($2n$ = 80, FN = 114; Patton *et al.*, 2000) and high genetic divergence (Cyt*b* K2P: 5.6–8.6%). It was also recovered as a distinct species within Clade A by both coalescent-based delimitation methods.

Oecomys bicolor/*O. cleberi* species group (Clade B) – six *O. bicolor* clades and two *O. cleberi* clades can be recognized:

(iv) *Oecomys bicolor* clades: specimens treated as *O. bicolor* were recovered in six distinct lineages (Cyt*b* K2P: 3.3–6.9%) with unresolved phylogenetic relationships. These specimens are represented by few localities, similar karyotypes ($2n$ = 80, FN = 140; see also Patton *et al.*, 2000) and variable morphology, which did not allow us to distinguish inter- or intraspecific variation. Thus, we suggest treating them provisionally as part of the *O. bicolor* species complex, until more adequate sampling and analyses are available. The use of the name *Oecomys bicolor* (Tomes, 1860) for these lineages is in accordance with the morphology described for samples from Amazonian specimens treated as *O. bicolor* by Smith & Patton (1999), Patton *et al.* (2000) and Rocha *et al.* (2012). Additional evidence regarding karyotype data also suggests that *O. bicolor* could represent a species complex; Gardner & Patton (1976) found $2n$ = 80, FN = 134 and 136 for specimens treated as *O. bicolor* from Loreto, Peru, while Gomes Júnior *et al.* (2016) reported $2n$ = 80, FN = 142 for *O. bicolor* specimens from Rios Jatapu and Purus, Amazonas, Brazil. These distinct karyotypes may represent distinct species. Moreover, previous molecular analyses have indicated *O. bicolor* as a species complex (Patton *et al.*, 2000; Andrade & Bonvicino, 2003; Rocha *et al.*, 2015). Gomes Júnior *et al.* (2016) also recovered three distinct lineages within specimens treated as *O. bicolor* from the Amazon biome (using cytochrome oxidase subunit 1 as the mtDNA marker), which could represent some of the distinct lineages recovered here.

(v) *Oecomys cleberi* clades: two clades, central and northwestern, are proposed based on our integrative data. Specimens from the central clade (Cyt*b* K2P: 3.2–8.2%) are distributed in the Cerrado biome and exhibit morphological and cytogenetic data ($2n$ = 80, FN = 124 and 134) distinguishable from those of other lineages in Clade B. The use of the name *Oecomys cleberi* Locks, 1981 for specimens recovered in the central clade is justified based on molecular, morphological and distributional data, which are in accordance with the holotype and other related specimens recovered in the central clade (MN 24131; Rocha *et al.*, 2012). We report a karyotype with $2n$ = 80, FN = 134 for *O. cleberi*, which is similar to the description by Gardner & Patton (1976) from Peru (MVZ 136592). Additionally, specimens with $2n$ = 80, FN = 124 (Andrades-Miranda *et al.*, 2001) are part of the *O. cleberi* central clade. Thus, this species can be characterized by $2n$ = 80 and FN = 124 and 134.

Specimens from the northwestern clade exhibited similar molecular data in relation to the *O. cleberi* central clade (Cyt*b* K2P: 0.5–2.9%). However, these specimens were recovered as a distinct species by three delimitation methods and had a similar karyotype and morphology to the specimens treated here as *O. bicolor*. *Oecomys cleberi* was previously considered a Cerrado endemic (Rocha *et al.*, 2012) and, as such, has one of the endemism patterns typical of the open biomes of South America, that is, it represents a vicariant species within a lineage that is well diversified in rainforest habitats (Carmignotto, de Vivo & Langguth, 2012). However, since we found Amazonian representatives (northwestern clade) strongly related to *O. cleberi* (central clade) and these clades were derived from *O. bicolor* clades, this could imply initial molecular differentiation from *O. bicolor* lineages (for *O. cleberi* northwestern clade) with subsequent morphological and cytogenetic differentiation (for *O. cleberi* central clade). Some rodent species currently distributed in Amazonia and Cerrado are strongly structured by differentiation resulting from geographic features such as river courses and interfluvials, which may have interrupted gene flow as recently as the late Pleistocene (Leite & Rogers, 2013). Moreover, an historical bridge between the Amazon basin, Cerrado and the Atlantic Forest has played an important role in the diversification of small mammal species, such as via the gallery forests along rivers of the central Brazilian Cerrado (Costa, 2003). Because specimens from the *O. bicolor* complex and *O. cleberi* northwestern clade inhabit the Amazon biome, this area could represent the ancestral area of *O. cleberi* diversification. Although *Oecomys* dispersion and differentiation from the Amazon to the Cerrado could be

hypothesized, additional analyses with samples from southern Amazonia and eastern Bolivia are required to test this hypothesis and clarify the taxonomic status of specimens of the *O. cleberi* northwestern clade.

Oecomys mamorae / *Oecomys franciscorum* species group (Clade C) – composed of three *O. mamorae* clades and the *O. franciscorum* clade:

(vi) *Oecomys mamorae* clades: specimens treated as part of *O. mamorae* species complex were recovered as three distinct lineages. They were indicated as three distinct species by delimitation methods, even though their phylogenetic relationships were not resolved in the Cyt*b* data set. Since these specimens have no cytogenetic data and we did not examine their morphology, we support the hypothesis advanced by previous studies. Carleton *et al.* (2009) examined the morphology of specimens from western Brazil, eastern Paraguay and western and central Bolivia, treating them as *O. mamorae*. Pardiñas *et al.* (2016) treated specimens from northwestern Bolivia as *O. mamorae* and specimens from central Bolivia, eastern Paraguay and western Brazil as *Oecomys* cf. *mamorae*. Since the type locality of *O. mamorae* (Thomas, 1906) was restricted to '…Muchanes, with approximate coordinates 15.18°S and 67.58°W, on the right forested side of the Beni River, department of Beni, Bolivia', the concept of *O. mamorae* was 'limited to the Bolivian populations that inhabit the riverine forest of the Amazonian drainage and the Yungas, excluding Bolivian and Paraguayan samples from Chiquitano and Chaco biomes'. This seems plausible since the three lineages, here treated as the *O. mamorae* complex, occur in distinct habitats (Yungas, western clade; Chiquitano and Chaco, southern clade; Pantanal, eastern clade) and have high molecular divergence (Cyt*b* K2P: 4.7–5.9%). This complex possibly represents three distinct cryptic species – see Carleton *et al.* (2009) and Pardiñas *et al.* (2016) for *O. mamorae* morphological analyses. Thus, the taxonomic status of these samples remains uncertain pending additional morphological analyses coupled with molecular and cytogenetic data.

(vii) *Oecomys franciscorum* clade: this clade was recently studied by Pardiñas *et al.* (2016). Here, we included four new sequences, including two from a new locality (Parque Nacional do Pantanal, Mato Grosso, Brazil), and the phylogenetic relationships recovered were similar to previous research, although the support was moderate (bootstrap: 70, BPP: 0.96). Pardiñas *et al.* (2016) treated samples from Brazil as *Oecomys* cf. *franciscorum* (previously reported as *Oecomys* sp. by Andrade & Bonvicino, 2003 and as *O. mamorae* by Percequillo *et al.*, 2011 and Rocha *et al.*, 2011). Although the delimitation methods pointed to four distinct species within this lineage, we considered all specimens as a single species, *O. franciscorum* Pardinãs *et al.*, 2016 based on molecular (Cyt*b* K2P: 0.0–1.1%), morphological and habitat similarity within specimens recovered in this group. Although we did not examine the holotype of *O. franciscorum*, the morphological characters examined here were similar to the description provided by Pardiñas *et al.* (2016). Additionally, this taxon was described as endemic to Humid Chaco (Orozco *et al.*, 2014 cited as *Oecomys* sp.; Pardiñas *et al.*, 2016), and specimens from Brazil are restricted to the Pantanal biome, which is also a humid environment. Two sequences karyotyped ($2n$ = 72, FN = 90; Andrade & Bonvicino, 2003) were recovered as part of the *O. franciscorum* clade, supporting the previous association of this diploid number with this lineage (Pardiñas *et al.*, 2016).

Oecomys paricola species group (Clade D) – composed of three distinct clades:

(viii) *Oecomys paricola* northern clade: represented by specimens from Ilha do Marajó, Pará State, Brazil. These specimens were revealed as a distinct species by the delimitation methods and were quite distinct from other *O. paricola* clades, both molecularly (Cyt*b* K2P: 2.9–4.3%) and cytogenetically ($2n$ = 70, FN = 72). Since we did not examine voucher specimens from the northern clade, we followed Rosa *et al.* (2012), who treated these specimens as a distinct species. This taxonomic assignment was based on the molecular divergence and structure, a distinct karyotype and 'consistent morphological differences between the populations from the Belém region and Marajó Island' found by Rosa *et al* (2012).

(ix) *Oecomys paricola* eastern clade: composed of specimens from Cerrado and recovered as a distinct lineage in molecular analyses. These specimens also showed distinct karyotypes ($2n$ = 68, FN = 72 and $2n$ = 70, FN = 76), allopatric geographic distribution and differences in size and qualitative morphological characters that warrant a specific taxonomic status. The use of the name *O. paricola* (Thomas, 1904) for specimens recovered in the eastern clade follows previous morphological descriptions (e.g. Rocha *et al.*, 2011; Rosa *et al.*, 2012; Carleton &

Musser, 2015). Specimens near the type locality (Igarapé-Açú, Pará, Brazil) were also recovered in the eastern clade (Barcarena, Pará, Brazil), which reinforces the name attribution as *O. paricola* for specimens distributed in northern Cerrado and the eastern Amazon.

(x) *Oecomys paricola* western clade: composed of specimens from the southern Amazon, which were recovered as a distinct and divergent lineage (Cyt*b* K2P: 4.7–6.2%). In fact, this clade was recovered as two sister lineages with high statistical support. These lineages were also quite divergent (Cyt*b* K2P: 2.2–2.9%), indicating two distinct species in delimitation methods. Nevertheless, geographic distribution, qualitative morphological characters and karyotype data were inconclusive, since we examined only one young specimen and it has only diploid number ($2n$ = 70, M97109) hampering comparisons. We therefore treat specimens recovered in the western clade as a distinct and single species in the *O. paricola* complex.

Oecomys catherinae species group (Clade E) – despite the great morphological similarity found among the specimens of Clade E, species delimitation analyses, molecular divergence (Cyt*b* K2P: 1.6–8.7%) and cytogenetic and distributional data support the hypothesis of five distinct taxa within this clade:

(xi) *Oecomys catherinae* western clade: composed of specimens from the southern Amazon that diverged early within Clade E (Cyt*b* K2P: 7.2–8.7%). They also exhibit the most distinct morphology within specimens from Clade E. Specimens recovered in the western clade had a distinct and new karyotype for the genus with $2n$ = 54, FN = 54, which corroborates its assignment as a valid species under *Oecomys*.

The other four lineages were recovered in a highly supported clade (bootstrap = 83.9% and BPP = 0.99) composed of four distinct and highly supported lineages:

(xii) *Oecomys catherinae* westernmost clade: represented by specimens from the southwestern Amazon that co-occur with specimens from the western clade (in Aripuanã, Mato Grosso State, Brazil). However, they are molecularly (Cyt*b* K2P: 3.7–4.9%), karyotypically ($2n$ = 60, FN = 62) and morphologically distinct from the other lineages, which provides evidence of their taxonomic distinctiveness.

(xiii) *Oecomys catherinae* eastern, (xiv) *O. catherinae* central and (xv) *O. catherinae* northern clades: despite the molecular similarity within these three lineages (Cyt*b* K2P 1.6–3.1%), they were recovered in three moderate to highly supported clades, with some distinct morphological traits. Moreover, they occur in distinct biomes, with specimens from the eastern clade restricted to the Atlantic Forest, those from central clade distributed in the Cerrado and specimens from the northern clade occurring in the eastern Amazon. This suggests specific taxonomic status for representatives of each clade. Additionally, specimens from the northern clade exhibit a new karyotype for the genus ($2n$ = 62, FN = 62) that is distinct from the eastern and central clade specimens ($2n$ = 60, FN = 62). The phylogenetic relationships recovered also suggest that $2n$ = 62 (northern clade) could arise through a chromosome fission rearrangement of the large submetacentric present in karyotypes with $2n$ = 60 (eastern and central clade – compare chromosome 1 in Figs 4G, H).

Oecomys catherinae Thomas, 1909 has been applied to large-sized specimens of *Oecomys* with grey-based and white tipped ventral hairs from the Atlantic Forest and Cerrado (Asfora *et al.*, 2011; Carleton & Musser, 2015). Thus, we treated specimens from Clade E with these morphological traits and geographic distribution as part of the *O. catherinae* complex. However, since we considered five distinct species in Clade E, and the type locality of *O. catherinae* is in southeastern Brazil (Joinville, Santa Catarina), we restricted this name to specimens recovered in the eastern clade distributed in the Atlantic Forest biome with $2n$ = 60, FN = 62.

Mitonuclear discordance was detected in Clade E: two nuclear markers recovered the Atlantic forest lineage (eastern clade) as the sister to western clade, but in Cyt*b* analyses, the eastern clade was recovered as the sister to the central and northern clades. Examples of mitonuclear discordance reviewed by Currat *et al.* (2008), Petit & Excoffier (2009) and Toews & Brelsford (2012) have often been attributed to introgressive hybridization. In this case, however, this phenomenon seems unlikely since the Atlantic Forest specimens exhibit $2n$ = 60 instead of $2n$ = 57 and 58, which would be expected in hybrids between the western clade ($2n$ = 54) and other lineages ($2n$ = 60 and 62). Incongruence among gene trees can also be explained by incomplete lineage sorting, selection or distinct mutation rates in specific genes (Jennings & Edwards, 2005; Pollard *et al.*, 2006; Syring *et al.*, 2007). The karyotype with $2n$ = 60, FN = 62 obtained for specimens from the central, eastern and westernmost clades was identical to those reported for *O. concolor* from Colombia (Gardner & Patton, 1976), for *Oecomys* cf. *concolor* from central Brazil (Andrades-Miranda *et al.*, 2001; Andrade & Bonvicino, 2003), for *O. catherinae* from northeastern Brazil (treated as *O. bahiensis*

by Langguth *et al.*, 2005) and for *O. catherinae* from southeastern and northeastern Brazil (Asfora *et al.*, 2011). Despite the position advocated by Asfora *et al.* (2011), who treated specimens reported as *Oecomys* cf. *concolor* (Andrades-Miranda *et al.*, 2001; Andrade & Bonvicino, 2003) from the Cerrado and those from the Atlantic Forest as *O. catherinae*, the phylogenetic and species delimitation analyses suggest the existence of distinct species with similar karyotypes in these distinct biomes. Moreover, sequences treated as *Oecomys* cf. *concolor* from the Brazilian Amazon and Cerrado reported by Miranda *et al*. (unpublished data) and as *O. rex* from the Brazilian Amazon by Pardiñas *et al.* (2016) were recovered in distinct clades, which reinforces that Clade E represents a species complex. Therefore, in this clade, karyotypic data are not adequate to distinguish species and it is necessary to combine phylogenetic analyses and geographic distribution to determine each taxon's identity.

More detailed analysis based on morphological variation and examination of type specimens will be required for assignment of the appropriate name to each new species delimited in this study. The species delimitation hypotheses that we have postulated for the genus *Oecomys* are based on the congruence among molecular phylogeny, species delimitation methods, karyology, geographic distribution and morphology. We were able to delimit 15 species (Clades A–E), with at least eight putative new species: two in the *O. roberti* species group (eastern and western clades), two in the *O. paricola* species group (northern and western clades) and four in the *O. catherinae* species group (central, northern, western and westernmost clades). Additionally, the high molecular divergence resulting in the multiple species recovered by the coalescence-based delimitation methods, along with the distinct karyotypic data, also suggest a higher cryptic diversity within the complexes of *O. bicolor*, *O. cleberi* and *O. mamorae*.

Evolutionary trends within the genus *Oecomys*

The evaluation of morphological traits throughout the trees we recovered allows us to infer some evolutionary trends in the genus *Oecomys*. One of them is the ventral colouration, as all taxa of Clades A, B and C are characterized by self-coloured white/yellowish venters versus grey-based hairs in the other lineages (Clades D and E). This suggests a single origin of venters with self-coloured hairs versus multiple origins for grey-based hairs in the ventral region. Additionally, Clades A and C are characterized by specimens with intermediate to large size, versus small to intermediate size in Clades B and D, while the species of clade E are larger, suggesting the importance of size in the evolutionary relationships within *Oecomys*. Weksler (2006) had already pointed to a medium-sized rat as an ancestral condition in oryzomyines, where small and large sizes represent the classes with a higher number of transformations from this intermediate size '*Bauplan*'. Additionally, Avaria-Llautureo *et al.* (2012), used a similar data set to Weksler (2006) and Percequillo *et al.* (2011) – IRBP and Cyt*b* genes – to recover a similar topology and hypothesized that the small size is the ancestral state and that size increased along the evolutionary lineages within Oryzomyini accordingly to Cope's rule (Rensch, 1948; Hone & Benton, 2005). Despite the putative body size of the ancestral lineages (medium or small), these contributions suggested an increase in size through evolutionary time in this tribe, perhaps explaining the trend we observed in *Oecomys*.

The diploid numbers of *Oecomys* have ranged from 54 to 86 (Patton *et al.*, 2000). In this study, we described three new karyotypes: $2n = 54$ (FN = 54), $2n = 62$ (FN = 62) and $2n = 70$ (FN = 74). The first one is the lowest diploid number for the genus together with that recently described for *O. rutilus* ($2n = 54$, FN = 82–90; Gomes Júnior *et al.*, 2016). Although diploid number can be used to distinguish some species of *Oecomys* (e.g. *Oecomys* sp. 2, *O. paricola*, *O. rutilus* and *O. trinitatis*), taxonomic identification required more detailed karyotype information such as fundamental number (e.g. *O. bicolor*, *O. cleberi* and *O. roberti*), geographic information and phylogenetic analyses (e.g. *O. catherinae* complex) in the majority of cases. A bidirectional trend of karyotype evolution of *Oecomys* could be inferred based on the phylogenetic relationships recovered in Figure 2; Clades A–D retained diploid numbers similar or higher than $2n = 70$ versus $2n = 62$ or lower than Clade E. Although our data preclude inferences regarding the ancestral diploid number in this bidirectional evolution, Langguth *et al.* (2005) suggested $2n = 60$, FN = 62 as the ancestral karyotype for the genus. The authors based their assumption on the widespread distribution of this karyotype, from Colombia to southeastern Brazil, and suggested that the distinct karyotypes might have evolved through Robertsonian rearrangements and pericentric inversions. Indeed, considering the range of diploid number and the remarkable sex chromosome variability, we could cite Robertsonian fusions/fissions, pericentric inversions, *in tandem* fusions/fissions and addition/deletion of constitutive heterochromatin in X- and Y-chromosomes as the most important events leading to karyotype diversity in *Oecomys*. Fluorescence *in situ* hybridization and chromosome painting have demonstrated that *in tandem* fusions and fissions, reciprocal translocations and paracentric inversions are much more common in rodents than previously thought (Hass, Sbalqueiro & Muller, 2008; Ventura *et al.*, 2009; Romanenko *et al.*, 2012; Di-Nizo *et al.*, 2015).

A high level of sympatry in the genus *Oecomys* was observed, as up to four species from different species groups were found at the same localities in Mato Grosso State, Brazil: *O. bicolor*, *O. paricola*, *O. roberti* and *O. catherinae* from Cláudia; *O. bicolor* and *O. roberti* from Apiacás; and *O. cleberi* and *O. catherinae* from Aripuanã. Sympatry in *Oecomys* has already been documented in the literature, either in catalogues (Cabrera, 1961; Carleton & Musser, 2015), taxonomic studies (Woodman *et al.*, 1991; Carleton *et al.*, 2009) or inventories (Patton *et al.*, 2000; Voss *et al.*, 2001; Hice & Velazco, 2012). Sympatry of congeneric species is unusual among sigmodontines and within the tribe Oryzomyini, few genera exhibit sympatry on species level (see Prado & Percequillo, 2013): for instance, species of the genera *Euryoryzomys* (*E. macconnelli* and *E. nitidus* in western Amazon, and *E. macconnelli* and *E. emmonsae* in eastern Amazon), *Hylaeamys* (*H. yunganus* and *H. perenensis* in western Amazon, and *H. yunganus* and *H. megacephalus* in eastern Amazon) and *Cerradomys* (*C. scotti* sympatric to *C. subflavus* in Atlantic Forest, and to *C. maracajuensis* or *C. marinhus* in Cerrado) (Patton, Pardiñas & D'Elía, 2015). All these groups are predominantly terrestrial, which raises the following question: is arboreality somehow related to the high levels of sympatry in *Oecomys*? We suggest two hypotheses: (1) assuming that vertical stratification of the forested habitats could be used in different ways by arboreal and scansorial mammals (Hildebrand, 1995; Galetti *et al.*, 2016), the accommodating sympatric species of *Oecomys* would exploit the diversity of arboreal substrates and resources and (2) sympatry could represent areas of secondary contact or expansion zones of species with different geographic origins, as proposed for other Neotropical species (Hughes & Eastwood, 2006; Antonelli *et al.*, 2009; Erkens, Maas & Couvreur, 2009; Condamine *et al.*, 2012). The patterns we recovered show that the sympatric species belong roughly to distinct 'size-groups', such as the small *O. bicolor*, intermediately sized *O. paricola* and *O. roberti* and large *O. catherinae*. However, there is no available information on how these species occupy their habitats, whether they use the same forest strata or the same food items. On the other hand, because they belong to distinct clades, there is support for a hypothesis of secondary contact among species.

Looking for similar patterns of sympatry, we evaluated the distribution of other rodent taxa. Within the tribe Oryzomyini, *Oecomys* is the only lineage represented by arboreal specialization, thus precluding any comparison with other phylogenetically allied taxa. Within the subfamily Sigmodontinae, the Thomasomyini genus *Rhipidomys* is also an arboreal specialist, but its species are widely allopatric and parapatric (Tribe, 2015). The *incertae sedis* genus *Juliomys* currently harbours four species: *J. pictipes*, *J. ossitenuis*, *J. rimofrons* and *J. ximenezi*, which are predominantly sympatric. *Juliomys pictipes* and *J. ossitenuis* are also syntopic throughout their entire range on the Brazilian coast from Minas Gerais to Rio Grande do Sul, except for the western distribution of the former in Paraguay and Argentina; *J. rimofrons* is restricted to São Paulo and Minas Gerais, being sympatric to the two former species in this area; *J. ximenezi* is only known from the type locality, where *J. pictipes* and *J. ossitenuis* also occur (Christoff *et al.*, 2016). Thus, *Juliomys* is the arboreal sigmodontine with the second highest level of sympatry (three species), only lesser than *Oecomys* (four species). Indeed, the authors of *J. ximenezi* hypothesized that 'differential use of microhabitat' and 'distinct feeding habits' could explain the co-occurrence of these similar and closely related taxa (Christoff *et al.*, 2016). Curiously, there are other scansorial/arboreal lineages that are monotypic in Atlantic Forest, such as *Sooretamys angouya*, *Phaenomys ferrugineus* and *Drymoreomys albimaculatus*; not phylogenetic allied, these taxa are greatly sympatric (Patton *et al.*, 2015). The arboreal Atlantic Forest species of the genus *Phyllomys*, family Echimyidae, exhibit some sympatry (Leite, 2003; Leite & Loss, 2015), but species of the Amazonian genera *Dactylomys*, *Echimys*, *Isothrix*, *Mesomys* and *Toromys* are predominantly allopatric or parapatric (Patton *et al.*, 2015). Therefore, no previous research has produced a clear pattern relating arboreality and sympatry. To address a more comprehensive hypothesis, a better understanding of the ecological and evolutionary forces that led to the diversification of species under *Oecomys* is needed.

The imperfect understanding of the systematics of *Oecomys* has become apparent when certain groups are treated as species complexes. Although our new investigation contributes to a better understanding of the evolutionary diversification of *Oecomys*, the description of valid species and the refinement of their geographic distribution and phylogenetic relationships require further work.

ACKNOWLEDGEMENTS

This work was supported by Fundação de Amparo à Pesquisa do Estado de São Paulo (FAPESP) grants #2005/04557-3 and #2014/02885-5 for MJJS, #2011/20022-3 for APC, #2010/03969-4 for MVB and #2009/16001-9 for ARP; Conselho Nacional de Desenvolvimento Científico e Tecnológico (CNPq) grants #563320/2010-9, 484346/2011-3 and 457444/2012-6 for APC; Fondo Nacional de Desarrollo Científico y Tecnológico de Chile (FONDECYT, CONICYT) grant #3160328 for EYS-V. We thank Dr Miguel T. Rodrigues, Dr Mario de Vivo, Dr Leonora Pires Costa and Dr Cibele R. Bonvicino for providing samples, respectively,

from mammal tissue collections of the Instituto de Biociências (IB-USP) and Museu de Zoologia (MZUSP), Universidade de São Paulo, Universidade Federal do Espírito Santo (UFES), and Museu Nacional (MN) da Universidade Federal do Rio de Janeiro. We appreciate the comments made by Dr Jose J. Núñez, an anonymous reviewer, and Dr Ulyses F. J. Pardinãs, who significantly improved the manuscript. We appreciate the correction of the English language on the manuscript by Dr G. J. Kenagy. We also thank Karina Banci, Camilla Di-Nizo and Keila Almeida, who obtained some sequences for the molecular analyses.

REFERENCES

Andrade AFB, Bonvicino CR. 2003. A new karyological variant of *Oecomys* (Rodentia: Sigmodontinae) and its phylogenetic relationship based on molecular data. *Genome* **46:** 195–203.

Andrades-Miranda J, Oliveira LFB, Zanchin NIT, Mattevi MS. 2001. Chromosomal description of the rodent genera *Oecomys* and *Nectomys* from Brazil. *Acta Theriologica* **46:** 269–278.

Antonelli A, Nylander JAA, Persson C, Sanmartin I. 2009. Tracing the impact of the Andean uplift on Neotropical plant evolution. *Proceedings of the National Academy of Sciences of the United States of America* **106:** 9749–9754.

Asfora PH, Palma ART, Astúa D, Geise L. 2011. Distribution of *Oecomys catherinae* Thomas, 1909 (Rodentia: Cricetidae) in northeastern Brazil with karyotypical and morphometrical notes. *Biota Neotropica* **11:** 415–424.

Avaria-Llautureo J, Hernández CE, Boric-Bargetto D, Canales-Aguirre CB, Morales-Pallero B, Rodríguez-Serrano E. 2012. Body size evolution in extant Oryzomyini rodents: Cope's rule or miniaturization? *PLoS ONE* **7:** e34654.

Bazinet AL, Zwickl DJ, Cummings MP. 2014. A gateway for phylogenetic analysis powered by grid computing featuring GARLI 2.0. *Systematic Biology* **63:** 812–818.

Cabrera A. 1961. Catalogo de los mamiferos de America del Sur. *Revista del Museo Argentino de Ciencias Naturales Berardino Rivadavia* **4:** 309–732.

Carleton MD, Emmons LH, Musser GG. 2009. A new species of the rodent genus *Oecomys* (Cricetidae: Sigmodontinae: Oryzomyini) from Eastern Bolivia, with emended definitions of *O. concolor* (Wagner) and O. *mamorae* (Thomas). *American Museum Novitates* **3661:** 1–32.

Carleton MD, Musser GG. 2015. Genus *Oecomys* Thomas, 1906. In: Patton JL, Pardiñas UFJ, D'Elía G, eds. *Mammals of South America, volume 2: rodents*. Chicago: University of Chicago Press, 291–292.

Carmignotto AP, de Vivo M, Langguth A. 2012. Mammals of the Cerrado and Caatinga: distribution patterns of the tropical open biomes of Central South América. In: Patterson BD, Costa LP, eds. *Bones, clones, and biomes: the history and geography of recent Neotropical mammals*. Chicago: University of Chicago Press, 203–229.

Carpenter JW. 2012. *Exotic Animal Formulary*. St. Louis Missouri: Elsevier Health Sciences.

Carstens BC, Dewey TA. 2010. Species delimitation using a combined coalescent and information-theoretic approach: an example from North American *Myotis* bats. *Systematic Biology* **59:** 400–414.

Carstens BC, Pelletier TA, Reid NM, Satler JD. 2013. How to fail at species delimitation. *Molecular Ecology* **22:** 4369–4383.

Christoff AU, Vieira EM, Oliveira LR, Gonçalves JW, Valiati VH, Tomasi PS. 2016. A new species of *Juliomys* (Rodentia, Cricetidae, Sigmodontinae) from the Atlantic Forest of Southern Brazil. *Journal of Mammalogy* **97:** 1469–1482.

Condamine FL, Silva-Brandao KL, Kergoat GJ, Sperling FAH. 2012. Biogeographic and diversification patterns of Neotropical Troidini butterflies (Papilionidae) support a museum model of diversity dynamics for Amazonia. *BMC Evolutionary Biology* **12:** 82.

Costa LP. 2003. The historical bridge between the Amazon and the Atlantic Forest of Brazil: a study of molecular phylogeography with small mammals. *Journal of Biogeography* **30:** 71–86.

Currat M, Ruedi M, Petit RJ, Excoffier L. 2008. The hidden side of invasions: massive introgression by local genes. *Evolution* **62:** 1908–1920.

D'Elía G. 2003. Phylogenetics of Sigmodontinae (Rodentia, Muroidea, Cricetidae), with special reference to the akodont group, and with additional comments on historical biogeography. *Cladistics* **19:** 307–323.

Di-Nizo CB, Neves CL, Vilela JF, Silva MJ. 2014. New karyologycal data and cytotaxonomic considerations on small mammals from Santa Virgínia (Parque Estadual da Serra do Mar, Atlantic Forest, Brazil). *Comparative Cytogenetics* **8:** 11–30.

Di-Nizo CB, Ventura K, Ferguson-Smith MA, O'Brien PC, Yonenaga-Yassuda Y, Silva MJ. 2015. Comparative chromosome painting in six species of *Oligoryzomys* (Rodentia, Sigmodontinae) and the karyotype evolution of the genus. *PLoS ONE* **10:** e0117579.

Drummond AJ, Suchard MA, Xie D, Rambaut A. 2012. Bayesian phylogenetics with BEAUti and the BEAST 1.7. *Molecular Biology and Evolution* **29:** 1969–1973.

Edgar RC. 2004. MUSCLE: multiple sequence alignment with high accuracy and high throughput. *Nucleic Acids Research* **32:** 1792–1797.

Erkens RHJ, Maas JW, Couvreur TLP. 2009. From Africa via Europe to South America: migrational route of a species-rich genus of Neotropical lowland rain forest trees (*Guatteria*, Annonaceae). *Journal of Biogeography* **36:** 2338–2352.

Felsenstein J. 1985. Confidence limits on phylogenies: an approach using the bootstrap. *Evolution* **39:** 783–791.

Ford CE, Hamerton JL. 1956. A colchicine, hypotonic citrate, squash sequence for mammalian chromosomes. *Stain Technology* **31:** 247–251.

Freshney RI. 1986. *Animal cell culture: a practical approach*. Oxford: IRL Press.

Fujisawa T, Barraclough TG. 2013. Delimiting species using single-locus data and the Generalized Mixed Yule Coalescent approach: a revised method and evaluation on simulated data sets. *Systematic Biology* **62:** 707–724.

Galetti M, Rodarte RR, Neves CL, Moreira M, Costa-Pereira R. 2016. Trophic niche differentiation in rodents and marsupials revealed by stable isotopes. *PLoS ONE* **11:** e0152494.

Gardner AL, Patton JL. 1976. Karyotypic variation in Oryzomyine rodents (Cricetidae) with comments on chromosomal evolution in the Neotropical Cricetinae complex. *Occasional Papers of the Museum of Zoology – Louisiana State University* **49:** 1–48.

Geise L, Paresque R, Sebastião H, Shirai LT, Astúa D, Marroig G. 2010. Non-volant mammals, Parque Nacional do Catimbau, Vale do Catimbau, Buíque, state of Pernambuco, Brazil, with karyologic data. *Check List* **6:** 180–186.

Gomes Júnior RG, Schneider CH, de Lira T, Carvalho ND, Feldberg E, da Silva MN, Gross MC. 2016. Intense genomic reorganization in the genus *Oecomys* (Rodentia, Sigmodontinae): comparison between DNA barcoding and mapping of repetitive elements in three species of the Brazilian Amazon. *Comparative Cytogenetics* **10:** 401–426.

Harrington RC, Near TJ. 2012. Phylogenetic and coalescent strategies of species delimitation in snubnose darters (Percidae: Etheostoma). *Systematic Biology* **61:** 63–79.

Hass I, Sbalqueiro IJ, Müller S. 2008. Chromosomal phylogeny of four Akodontini species (Rodentia, Cricetidae) from Southern Brazil established by Zoo-FISH using *Mus musculus* (Muridae) painting probes. *Chromosome Research* **16:** 75–88.

Hershkovitz P. 1960. Mammals of northern Colombia, preliminary report no. 8: arboreal rice rats, a systematic revision of the subgenus *Oecomys*, genus *Oryzomys*. *Proceedings of the United States National Museum* **110:** 513–568.

Hershkovitz P. 1962. Evolution of Neotropical cricetine rodents (Muridae) with special reference to the phyllotine group. *Fieldiana: Zoology* **46:** 1–524.

Hice CL, Velazco PM. 2012. *The non-volant mammals of the Reserva Nacional Allpahuayo-Mishana, Loreto, Peru*. Lubbock: Museum of Texas Tech University.

Hildebrand M. 1995. *Analysis of vertebrate structure*. New York: John Wiley & Sons, Inc.

Hone DW, Benton MJ. 2005. The evolution of large size: how does Cope's Rule work? *Trends in Ecology & Evolution* **20:** 4–6.

Hughes C, Eastwood R. 2006. Island radiation on a continental scale: exceptional rates of plant diversification after uplift of the Andes. *Proceedings of the National Academy of Sciences of the United States of America* **103:** 10334–10339.

Irwin DM, Kocher TD, Wilson AC. 1991. Evolution of the cytochrome *b* gene of mammals. *Journal of Molecular Evolution* **32:** 128–144.

Jennings WB, Edwards SV. 2005. Speciational history of Australian grass finches (*Poephila*) inferred from thirty gene trees. *Evolution* **59:** 2033–2047.

Knowles LL, Carstens BC. 2007. Delimiting species without monophyletic gene trees. *Systematic Biology* **56:** 887–895.

Kubatko LS, Carstens BC, Knowles LL. 2009. STEM: species tree estimation using maximum likelihood for gene trees under coalescence. *Bioinformatics (Oxford, England)* **25:** 971–973.

Lanfear R, Calcott B, Ho SY, Guindon S. 2012. Partitionfinder: combined selection of partitioning schemes and substitution models for phylogenetic analyses. *Molecular Biology and Evolution* **29:** 1695–1701.

Langguth A, Maia V, Mattevi M. 2005. Karyology of large size Brazilian species of the genus *Oecomys* Thomas, 1906 (Rodentia, Muridae, Sigmodontinae). *Arquivos do Museo Nacional de Rio de Janeiro* **63:** 183–190.

Leite RN, Rogers DS. 2013. Revisiting Amazonian phylogeography: insights into diversification hypotheses and novel perspectives. *Organisms Diversity & Evolution* **13:** 639–664.

Leite YL, Loss AC. 2015. Genus *Phyllomys* Lund, 1839. In: Patton JL, Pardiñas UFJ, D'Elía G, eds. *Mammals of South America, volume 2: rodents*. Chicago: University of Chicago Press, 291–292.

Leite YLR. 2003. Evolution and systematics of the Atlantic tree rats, genus *Phyllomys* (Rodentia, Echimyidae), with description of two new species. Berkeley: University of California Press.

Maddison WP, Maddison DR. 2011. Mesquite: a modular system for evolutionary analysis. Available at: http://mesquiteproject.org

Matocq MD, Shurtliff QR, Feldman CR. 2007. Phylogenetics of the woodrat genus *Neotoma* (Rodentia: Muridae): implications for the evolution of phenotypic variation in male external genitalia. *Molecular Phylogenetics and Evolution* **42:** 637–652.

Musser GG, Carleton MD. 1993. Family Muridae. In: Wilson DE, Reeder DAM, eds. *Mammal species of the world: a taxonomic and geographic reference*. 2nd ed. Washington: Smithsonian Institution Press, 501–755.

Musser GG, Carleton MD. 2005. Order Rodentia. In: Wilson DE, Reeder DAM, eds. *Mammal species of the world: a taxonomic and geographic reference*. 3rd ed. Baltimore: The Johns Hopkins University Press, 745–752.

Nabholz B, Mauffrey JF, Bazin E, Galtier N, Glemin S. 2008. Determination of mitochondrial genetic diversity in mammals. *Genetics* **178:** 351–361.

O'Meara BC. 2010. New heuristic methods for joint species delimitation and species tree inference. *Systematic Biology* **59:** 59–73.

Olson DM, Dinerstein E, Wikramanayake ED, Burgess ND, Powell GVN, Underwood EC, D'Amico JA, Itoua I, Strand HE, Morrison JC, Loucks CJ, Allnutt TF, Ricketts TH, Kura Y, Lamoreux JF, Wettengel WW, Hedao P, Kassem KR. 2001. Terrestrial ecoregions of the world: a new map of life on earth. *Bioscience* **51:** 933–938.

Orozco MM, Piccinali RV, Mora MS, Enriquez GF, Cardinal MV, Gürtler RE. 2014. The role of sigmodontine rodents as sylvatic hosts of *Trypanosoma cruzi* in the Argentinean Chaco. *Infection, Genetics and Evolution* **22:** 12–22.

Paglia AP, Fonseca GAB, Rylands AB, Herrmann G, Aguiar LMS, Chiarello AG, Leite YLR, Costa LP, Siciliano S, Kierulff MCM, Mendes SL, Tavares VC, Mittermeier RA, Patton JL. 2012. *Lista Anotada dos Mamíferos do Brasil*. Arlington: Conservation International.

Pardiñas UFJ, Teta P, Salazar-Bravo J, Myers P, Galliari CA. 2016. A new species of arboreal rat, genus *Oecomys*

(Rodentia, Cricetidae) from Chaco. *Journal of Mammalogy* **97:** 1177–1196.

Paresque R, Silva MJJ, Yonenaga-Yassuda Y, Fagundes V. 2007. Karyological geographic variation of *Oligoryzomys nigripes* Olfers, 1818 (Rodentia, Cricetidae) from Brazil. *Genetics and Molecular Biology* **30:** 43–53.

Patton JL, Da Silva MNF. 1995. A review of the spiny mouse genus *Scolomys* (Rodentia, Muridae, Sigmodontinae) with the description of a new species from the western Amazon of Brazil. *Proceedings of the Biological Society of Washington* **108:** 319–337.

Patton JL, Da Silva MNF, Malcolm JR. 2000. Mammals of the Rio Juruá and the evolutionary and ecological diversification of Amazonia. *Bulletin of the American Museum of Natural History* **244:** 1–306.

Patton JL, Pardiñas UFJ, D'Elía G. 2015. *Mammals of South America, volume 2: rodents*. Chicago: University of Chicago Press.

Percequillo AR, Weksler M, Costa LP. 2011. A new genus and species of rodent from the Brazilian Atlantic Forest (Rodentia: Cricetidae: Sigmodontinae: Oryzomyini), with comments on oryzomyine biogeography. *Zoological Journal of Linnean Society* **161:** 357–390.

Pereira LG, Geise L. 2007. Karyotype composition of some rodents and marsupials from Chapada Diamantina (Bahia, Brasil). *Brazilian Journal of Biology* **67:** 509–518.

Petit RJ, Excoffier L. 2009. Gene flow and species delimitation. *Trends in Ecology & Evolution* **24:** 386–393.

Pine RH, Timm RM, Weksler M. 2012. A newly recognized clade of trans-Andean Oryzomyini (Rodentia: Cricetidae), with description of a new genus. *Journal of Mammalogy* **93:** 851–870.

Pollard DA, Iyer VN, Moses AM, Eisen MB. 2006. Widespread discordance of gene trees with species tree in *Drosophila*: evidence for incomplete lineage sorting. *PLoS Genetics* **2:** e173.

Pons J, Barraclough TG, Gomez-Zurita J, Cardoso A, Duran DP, Hazell S, Kamoun S, Sumlin WD, Vogler AP. 2006. Sequence-based species delimitation for the DNA taxonomy of undescribed insects. *Systematic Biology* **55:** 595–609.

Prado JRD, Percequillo AR. 2013. Geographic distribution of the genera of the tribe Oryzomyini (Rodentia: Cricetidae: Sigmodontinae) in South America: patterns of distribution and diversity. *Arquivos de Zoologia* **44:** 1–120.

Rambaut A, Suchard M, Xie D, Drummond A. 2014. Tracer. Available at: http://tree.bio.ed.ac.uk/software/tracer/

Rannala B. 2015. The art and science of species delimitation. *Current Zoology* **61:** 846–853.

Rannala B, Yang Z. 2003. Bayes estimation of species divergence times and ancestral population sizes using DNA sequences from multiple loci. *Genetics* **164:** 1645–1656.

Reid NM, Carstens BC. 2012. Phylogenetic estimation error can decrease the accuracy of species delimitation: a Bayesian implementation of the general mixed Yule-coalescent model. *BMC Evolutionary Biology* **12:** 196.

Rensch B. 1948. Histological changes correlated with evolutionary changes of body size. *Evolution* **2:** 218–230.

Rocha RG, Ferreira E, Costa BMA, Martins ICM, Leite YLR, Costa LP, Fonseca C. 2011. Small mammals of the mid-Araguaia River in central Brazil, with the description of a new species of climbing rat. *Zootaxa* **2789:** 1–34.

Rocha RG, Ferreira E, Fonseca C, Justino J, Leite YL, Costa LP. 2014. Seasonal flooding regime and ecological traits influence genetic structure of two small rodents. *Ecology and evolution* **4:** 4598–4608.

Rocha RG, Fonseca C, Zhou Z, Leite YLR, Costa LP. 2012. Taxonomic and conservation status of the elusive *Oecomys cleberi* (Rodentia, Sigmodontinae) from central Brazil. *Mammalian Biology* **77:** 414–419.

Rocha RG, Justino J, Leite YLR, Costa LP. 2015. DNA from owl pellet bones uncovers hidden biodiversity. *Systematics and Biodiversity* **13:** 403–412.

Romanenko SA, Perelman PL, Trifonov VA, Graphodatsky AS. 2012. Chromosomal evolution in Rodentia. *Heredity* **108:** 4–16.

Ronquist F, Huelsenbeck JP. 2003. MrBayes 3: Bayesian phylogenetic inference under mixed models. *Bioinformatics (Oxford, England)* **19:** 1572–1574.

Rosa CC, Flores T, Pieczarka JC, Rossi RV, Sampaio MI, Rissino JD, Amaral PJ, Nagamachi CY. 2012. Genetic and morphological variability in South American rodent *Oecomys* (Sigmodontinae, Rodentia): evidence for a complex of species. *Journal of Genetics* **91:** 265–277.

Smith M, Patton J. 1999. Phylogenetic relationships and the radiation of sigmodontine rodents in South America: evidence from cytochrome *b*. *Journal of Mammalian Evolution* **6:** 89–128.

Smith MF, Patton JL. 1993. The diversification of South American murid rodents: evidence from mitochondrial DNA sequence data for the Akodontine tribe. *Biological Journal of the Linnean Society* **50:** 149–177.

Stanhope MJ, Czelusniak J, Si JS, Nickerson J, Goodman M. 1992. A molecular perspective on mammalian evolution from the gene encoding interphotoreceptor retinoid binding protein, with convincing evidence for bat monophyly. *Molecular Phylogenetics and Evolution* **1:** 148–160.

Sukumaran J, Knowles LL. 2017. Multispecies coalescent delimits structure, not species. *Proceedings of the National Academy of Sciences* **114:** 1607–1612.

Sumner AT. 1972. A simple technique for demonstrating centromeric heterochromatin. *Experimental Cell Research* **75:** 304–306.

Syring J, Farrell K, Businský R, Cronn R, Liston A. 2007. Widespread genealogical nonmonophyly in species of *Pinus* subgenus *Strobus*. *Systematic Biology* **56:** 163–181.

Tamura K, Stecher G, Peterson D, Filipski A, Kumar S. 2013. MEGA6: molecular evolutionary genetics analysis version 6.0. *Molecular Biology and Evolution* **30:** 2725–2729.

Thompson JD, Higgins DG, Gibson TJ. 1994. CLUSTAL W: improving the sensitivity of progressive multiple sequence alignment through sequence weighting, position-specific gap penalties and weight matrix choice. *Nucleic Acids Research* **22:** 4673–4680.

Toews DP, Brelsford A. 2012. The biogeography of mitochondrial and nuclear discordance in animals. *Molecular Ecology* **21:** 3907–3930.

Tribe CJ. 2015. Genus *Rhipidomys*. In: Patton JL, Pardiñas UFJ, D'Elía G, eds. *Mammals of South America, volume 2: rodents*. Chicago: University of Chicago Press, 291–292.

Ventura K, O'Brien PC, Yonenaga-Yassuda Y, Ferguson-Smith MA. 2009. Chromosome homologies of the highly rearranged karyotypes of four *Akodon* species (Rodentia, Cricetidae) resolved by reciprocal chromosome painting: the evolution of the lowest diploid number in rodents. *Chromosome Research* **17:** 1063–1078.

Vilela JF, Mello B, Voloch CM, Schrago CG. 2014. Sigmodontine rodents diversified in South America prior to the complete rise of the Panamanian Isthmus. *Journal of Zoological Systematics and Evolutionary Research* **52:** 249–256.

Voss RS. 1988. Systematics and ecology of Ichthyomyine rodents (Muroidea): patterns of morphological evolution in a small adaptive radiation. *Bulletin of the American Museum of Natural History* **188:** 260–493.

Voss RS, Lunde DP, Simmons NB. 2001. The mammals of Paracou, French Guiana: a Neotropical lowland rainforest fauna part 2. Nonvolant species. *Bulletin of the American Museum of Natural History* **263**: 3–236.

Walsh PS, Metzger DA, Higuchi R. 1991. Chelex 100 as a medium for simple extraction of DNA for PCR-based typing from forensic material. *Biotechniques* **10:** 506–513.

Weksler M. 2003. Phylogeny of Neotropical oryzomyine rodents (Muridae: Sigmodontinae) based on the nuclear IRBP exon. *Molecular Phylogenetics and Evolution* **29:** 331–349.

Weksler M. 2006. Phylogenetic relationships of oryzomine rodents (Muroidea, Sigmodontinae): separate and combined analyses of morphological and molecular data. *Bulletin of the American Museum of Natural History* **296:** 1–149.

Weksler M. 2015. Tribe Oryzomyini Vorontsov, 1959. In: Patton JL, Pardiñas UFJ, D'Elía G, eds. *Mammals of South America, volume 2: rodents*. Chicago: University of Chicago Press, 291–292.

Wiens JJ. 2007. Species delimitation: new approaches for discovering diversity. *Systematic Biology* **56:** 875–878.

Woodman NRM, Timm R, Arana CV, Pacheco CA, Schmidt ED, Hooper C, Pacheco A. 1991. Annotated checklist of the mammals of Cuzco Amazónico, Peru. *Occasional Papers of the Museum of Natural History, University of Kansas* **145:** 1–12.

Yang Z, Rannala B. 2010. Bayesian species delimitation using multilocus sequence data. *Proceedings of the National Academy of Sciences of the United States of America* **107:** 9264–9269.

Zhang J, Kapli P, Pavlidis P, Stamatakis A. 2013. A general species delimitation method with applications to phylogenetic placements. *Bioinformatics (Oxford, England)* **29:** 2869–2876.

APPENDIX I

List of specimens examined for cytogenetic analyses, their respective diploid and fundamental number and collection localities

Numbers are cited on the maps of Figure 3. AC, Acre; GO, Goiás; MG, Minas Gerais; MT, Mato Grosso; PI, Piauí; SP, São Paulo.

Clade A: *Oecomys roberti* species group: **2*n* = 82, FN = 106**: M968464 (Apiacás, MT: 36); MZUSP29526 (Cláudia, MT: 41).

Clade B: *Oecomys bicolor*/*O. cleberi* species group: **2*n* = 80, FN = 140**: MJJS68, MJJS69 (Antimary, AC: 11); MJJS351 (Serra das Galés, GO: 27); MZUSP29523 (Apiacás, MT: 36); MZUSP35534 (Aripuanã, MT: 38); MZUSP29528 (Cláudia, MT: 41). **2*n* = 80, FN = 134**: PCH3674 (Guará, SP: 61); PCH3617 (São Joaquim da Barra, SP: 62). **2*n* = 80**: MZUSP35536 (Aripuanã, MT: 38); MZUSP35544 (Cláudia, MT: 41); PCH3881, PCH4172, PCH4180, PCH4222 (Guará, SP: 61); PCH3741, PCH3913, PCH3993, PCH3997, PCH4062, PCH4377 (São Joaquim da Barra, SP: 62); UNB1716, UNB1917, UNB1955, MN71672, MN71688, MN71692 (PARNA Emas, GO: 26).

Clade D: *Oecomys paricola* species group: **2*n* = 70, FN = 76**: UU043 (ESEC Uruçui-Una, PI: 56). **2*n* = 70, FN = 74**: MZUSP29525, MZUSP29527 (Cláudia, MT: 41). **2*n* = 70**: M97109, M97148 (Cláudia, MT: 41).

Clade E: *Oecomys catherinae* species group: **2*n* = 54, FN = 54**: PEU960006, MZUSP29531 (Aripuanã, MT: 38); MZUSP35543 (Cláudia, MT: 41); MZUSP29516 (Gaúcha Norte, MT: 43); MZUSP35537 (Juruena, MT: 44). **2*n* = 60, FN = 62**: CIT2096, CIT2097 (P.E. Rio Doce, MG: 30); MZUSP29532, MZUSP35535 (Aripuanã, MT: 38); PCH 3998, PCH4077 (São Joaquim da Barra, SP: 62). **2*n* = 62, FN = 62**: APC292, APC297, MZUSP29533, MZUSP35538, MZUSP35539, MZUSP35542 (Vila Rica, MT: 48).

APPENDIX II

List of specimens examined for morphological features and their respective collection localities

Locality numbers are cited on the maps of Figure 3. *Specimens not sequenced but with similar morphology from nearby regions of the corresponding molecular clade.

Clade A: *Oecomys roberti* species group: central clade (n = 7): AMAZONAS: (14) Igarapé-Açu, Rio Abacaxis (fluid: MZUSP 35533). MATO GROSSO: (37) APM Manso, Rio Manso, Chapada dos Guimarães (skin/skull: APM 680, MZUSP 35547); (41) Cláudia (skin/skull: M 976310*, MZUSP 29526); (43) Gaúcha do Norte (skin/skull: M 001*); (47) UHE Guaporé, Vale de São Domingos (skin/skull: MZUSP 35548).

Clade B: *Oecomys bicolor* complex (n = 5): central clade (n = 1): MATO GROSSO: (36) Apiacás (skin/skull: MZUSP 29523). Southern clade (n = 4): MATO

GROSSO: (41) Cláudia (skin/skull: M 968571*, MZUSP 29528, MZUSP 29529*, MZUSP 35544). *Oecomys cleberi* complex (n = 9): northwestern clade (n = 2): MATO GROSSO: (38) Aripuanã (skin/skull: MZUSP 35534, fluid: MZUSP 35536). Central clade (n = 7): SÃO PAULO: (not mapped) Teodoro Sampaio (skin/skull: FPR 06*, FPR 07*); (61) Guará (skin/skull: PCH 4260*, PCH 4272*, PCH 4280*, PCH 4523*); (62) São Joaquim da Barra (skin/skull: PCH 4377).

Clade C: *Oecomys franciscorum* (n = 5): MATO GROSSO: (45) PARNA Pantanal (skin/skull: PNPA 285*, PNPA 297*, PNPA 298*, MZUSP 35540, MZUSP 35541).

Clade D: *Oecomys paricola* species group (n = 15): western clade (n = 6): MATO GROSSO: (41) Cláudia (skull: M 97148, skin/skull: M 97109, MZUSP 29525, MZUSP 29527, MZUSP 29530, MZUSP 35545). Eastern clade (n = 9): PIAUÍ: (56) ESEC Uruçuí-Una (skin/skull: MZUSP 30332, MZUSP 30333*, MZUSP 30334*, MZUSP 30335*, MZUSP 30340). TOCANTINS: (63) ESEC Serra Geral do Tocantins (skin/skull: APC 1251, MZUSP 35552, MZUSP 35553; MZUSP 35694; fluid: MZUSP 35551).

Clade E: *Oecomys catherinae* species group (n = 21): western clade (n = 5): MATO GROSSO: (38) Aripuanã (skin/skull: APC 265*, MZUSP 29531); (41) Cláudia (skin/skull: MZUSP 35543); (43) Gaúcha do Norte (skin/skull: MZUSP 29516); (44) Juruena (skin/skull: MZUSP 35537). Westernmost clade (n = 3): MATO GROSSO: (38) Aripuanã (skin/skull: APC 255*, MZUSP 29532, MZUSP 35535). Central clade (n = 4): SÃO PAULO: (62) São Joaquim da Barra (skin/skull: PCH 3998, PCH 4077). TOCANTINS: (66) Paranã (skin/skull: MZUSP 35549, MZUSP 35550). Northern clade (n = 8): MATO GROSSO: (48) Vila Rica (skin/skull: APC 292, APC 293*, APC 297, APC 313*, MZUSP 29533, MZUSP 35538, MZUSP 35539, MZUSP 35542). Eastern clade (n = 7): BAHIA: (not mapped) Maruim, Una (skin/skull: MZUSP 34327*, MZUSP 34376*). SÃO PAULO: (60) Parque Estadual Intervales, Capão Bonito (skin/skull: MVZ 182087*, MVZ 200982, MVZ 200983*, MVZ 200984*, MVZ 200985*, MVZ 200986*).

SUPPORTING INFORMATION

Additional Supporting Information may be found in the online version of this article at the publisher's web-site:

Figure S1. Maximum likelihood (ML) trees using mitochondrial (Cyt*b*) and nuclear (IRPB + iBF7) data sets. Bayesian inference (BI) showed the same topology. Bootstrap and posterior probability support values are shown above branches for values above 70% and/or above 0.90, respectively. Clades A–E are indicated. Note mitonuclear incongruence for samples from the Atlantic Forest in Clade E (CIT 2096, CIT 2097 and LBCE 10774; blue branches).

Table S1. Sequences from *Oecomys* species used in this study with localities and map numbers as indicated in Figure 3. Taxon, voucher, field number and its corresponding clade are indicated according to Figures 1 and 2. GenBank accession numbers and references are listed. States in Brazil (UF) were abbreviated as follows: Acre (AC), Amazonas (AM), Bahia (BA), Espírito Santo (ES), Goiás (GO), Maranhão (MA), Minas Gerais (MG), Mato Grosso do Sul (MS), Mato Grosso (MT), Pará (PA), Piauí (PI), Rio de Janeiro (RJ), Rondônia (RO), São Paulo (SP), and Tocantins (TO). Additionally, Distrito Federal (DF), Brasília.

Table S2. Sequences used in this study as outgroup. Taxon, gene, GenBank number, voucher /field number, localities and references are indicated. States in Brazil were abbreviated as in Supporting Information, Table S1.

Table S3. External and craniodental measurements (in millimetre) and weight (in grams) of adult *Oecomys* specimens analysed in this study.